Structures of Usher Syndrome 1 Proteins and Their Complexes

Lifeng Pan and Mingjie Zhang

Physiology 27:25-42, 2012. doi:10.1152/physiol.00037.2011

Physiology (formerly published as News in Physiological Science) publishes brief review articles on major physiological developments. It is published bimonthly in February, April, June, August, October, and December by the American Physiological Society, 9650 Rockville Pike, Bethesda MD 20814-3991. ISSN: 1548-9213, ESSN: 1548-9221. Visit our website at http://www.the-aps.org/.

PHYSIOLOGY 27: 25–42, 2012; doi:10.1152/physiol.00037.2011

Structures of Usher Syndrome 1 Proteins and Their Complexes

Lifeng Pan and Mingjie Zhang
Division of Life Science, State Key Laboratory of Molecular Neuroscience, Hong Kong University of Science and Technology, Clear Water Bay, Kowloon, Hong Kong
mzhang@ust.hk

Usher syndrome 1 (USH1) is the most common and severe form of hereditary loss of hearing and vision. Genetic, physiological, and cell biological studies, together with recent structural investigations, have not only uncovered the physiological functions of the five USH1 proteins but also provided mechanistic explanations for the hearing and visual deficiencies in humans caused by USH1 mutations. This review focuses on the structural basis of the USH1 protein complex organization.

As one of the five classical senses, hearing allows us to interact both with our environment and with human society, to enjoy the beauty of music, and to participate in interpersonal conversation; it is in all regards functionally essential to human society. Although the detailed mechanisms underlying hearing are very complicated and remain largely unknown, the basic principles of hearing are simple. Essentially, sound waves are detected by our ears, converted into neural signals, and then sent to our brains for interpretation. Each mammalian ear has three compartments: the external ear, the middle ear, and the inner ear. The external ear, or the pinna, collects sound waves and funnels them down the ear canal, where they cause the eardrum to vibrate. These vibrations are then carried through the ossicles of the middle ear into the cochlea, a snail-shaped organ in the inner ear that converts sound waves into neural signals through hair cells. These signals are then passed to brain via the auditory nervous system (30, 109) (FIGURE 1A). Hair cells, present in all vertebrates, are highly polarized epithelial cells containing sensory receptors (33). In mammals, there are ~15,000–30,000 neurosensory hair cells within the organ of Corti on a thin basilar membrane in the cochlea of the inner ear (34). They derive their name from the tufts of stereocilia, known as hair bundles, which protrude from their apical surfaces into a fluid-filled tube within the cochlea known as the scala media. As shown in FIGURE 1B, mammalian cochlear hair cells can be further divided into two anatomically and functionally distinct subtypes: the inner and outer hair cells. The inner hair cells transform sound vibrations in the fluid of the cochlea into electrical signals, which are relayed to the auditory brain stem and eventually to the auditory cortex through neurotransmitter release-induced action potentials in afferent neurons, whereas the outer hair cells mechanically amplify low-level sound that enters the cochlea, in addition to sending neural signals to the brain (9). This amplification may be powered by movements of their hair bundles or by electrically driven movements of their cell bodies (38, 53).

The response time of the auditory system is only a few microseconds, too short for the system to involve a second messenger (21); instead, hair cells use an elaborate mechanosensory organelle, the hair bundle, to respond to sound stimuli (52). Each hair bundle comprises a staircase-like structure called stereocilia, each of which is filled with ~100 polarized actin filaments (FIGURE 1C). The hair bundles of immature and vestibular hair cells also contain a microtubule-based kinocilium, which is coupled with stereocilia through the kinocilial links and is involved in the establishment of the planar cell polarity during the development of the hair bundles (34, 58). In mature hair bundles, stereocilia taper off at their bases and insert into the apical surfaces of hair cells to form structures called rootlets (FIGURE 1C) (36, 60). They are normally arranged in three to four rows of increasing height in a staircase-like manner; stereocilia in different rows are connected by many fibrous extracellular links, and the tallest row is directly linked with the tectorial membrane (10, 24, 77, 92, 108).

A tip link is a single, four-stranded link that connects the tip of one stereocilium to the side of the nearest taller stereocilium (84). Tip links are aligned along the functional axes of hair bundles, and their ends are anchored at electron-dense plaques on the membranes of stereocilia referred to as the upper tip-link density (UTLD) and the lower tip-link density (LTLD) (35). Tip links are detectable as early as E17 in mice and persist throughout life (37, 41). Tip links play important roles in hearing transduction, since they have been proposed to be coupled with mechanotransduction (MET) channels (38, 39, 51), which have been proved to be located at the bottoms of tip links (13). In response to sound stimuli, the hair bundle, including all stereocilia and the liquid between them, deflects and pivots in unison around the

basal insertion points of the stereocilia (62, 63). This results in changes in tension on tip links, which opens the coupled MET channels in the plasma membrane. The rapid influx of cations, mostly K^+ and Ca^{2+}, through the opened MET channels leads to hair cell depolarization, neurotransmitter release, and the eventual transmission of the auditory signal to the central nervous system (FIGURE 1D).

Hair cells can be lost or damaged by aging, noise exposure, ototoxic drugs such as aminoglycoside antibiotics, and mutant alleles of genes that are essential for hearing (31, 83). Human Usher syndrome (USH) is a severe hereditable sensorineural hearing impairment named after Charles Usher, a British ophthalmologist who described the hereditary nature of this disorder in retinitis pigmentosa (RP) patients. USH is the most common cause of

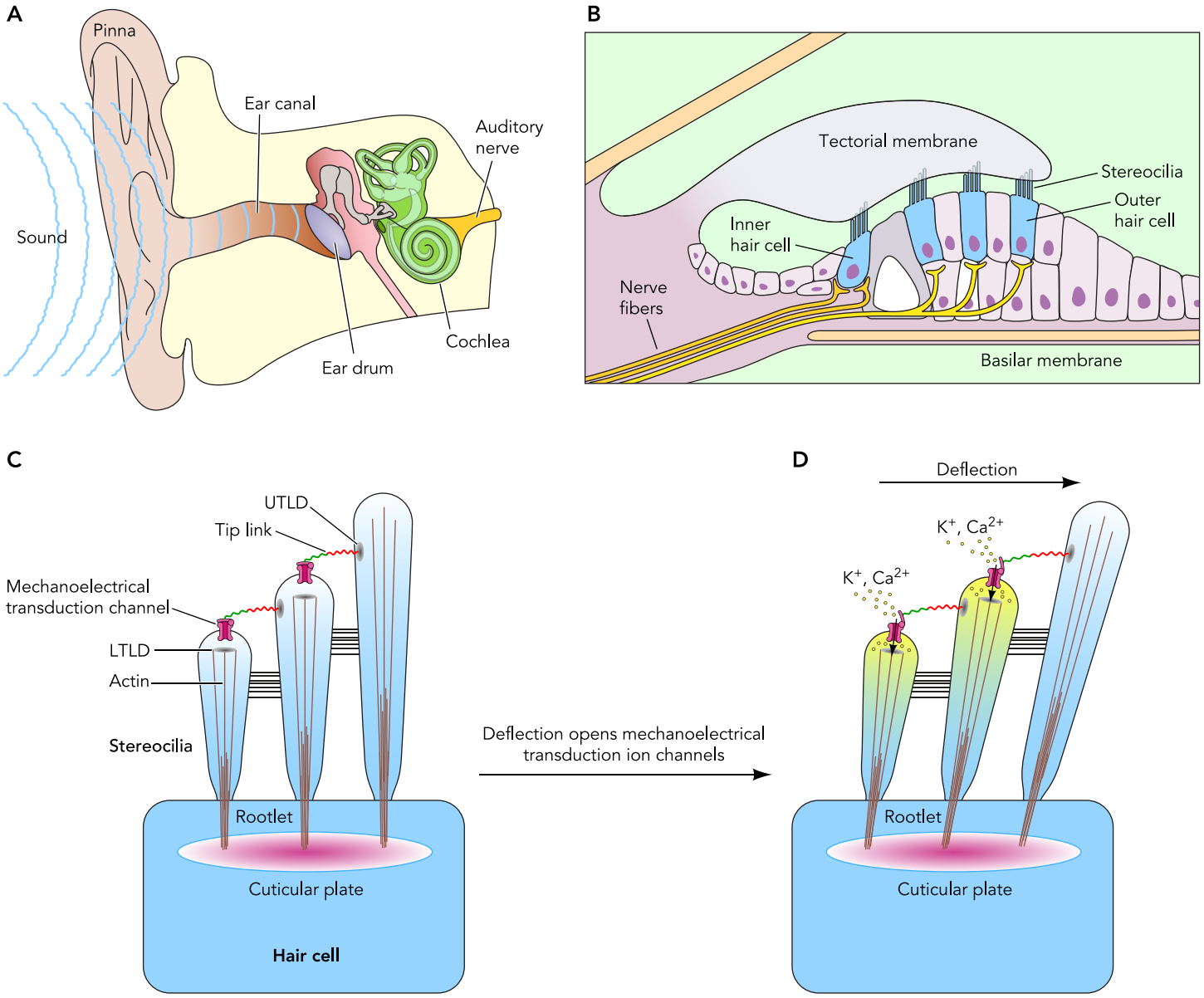

FIGURE 1. **Schematic drawing showing sound signal transductions in the mammalian ear**
A: schematic diagram showing the basic anatomy of a mammalian ear. Sound waves pass through the ear canal, vibrate the ear drum in the middle ear, and then transmit into the inner ear, where mechanical vibrations are converted into electrical nerve impulses by the snail-shaped organ called cochlea. Finally, the hearing signals are passed to brain via the auditory nerve system. *B*: a transverse section of the sensory part of cochlea, depicting the cellular structure of the sound-detecting organ. The cochlea has an assembly of intricately shaped supporting cells as well as inner and outer hair cells, which are supported by a flexible basilar membrane at one end and are connected with the tectorial membrane through their stereocilia at the other end. The sound vibrations cause displacement of the basilar membrane, which stimulates the hair cells by bending the stereocilia bundles against the tectorial membrane. *C*: schematic diagram showing a mature hair bundle of a mammalian hair cell. Stereocilia in a hair bundle are filled with polarized actin filaments with their plus ends pointing to the stereociliary tips and inserted into the apical surface of the hair cell to form the rootlets. Tip link is thought to gate the mechanoelectrical transduction channel and forms two unique anchor points along stereocilia: the upper tip-link density (UTLD) and the lower tip-link density (LTLD). *D*: sound-induced deflections of stereocilia induce tension on tip links, which somehow open the coupled mechanoelectrical transduction channel. Then ions, mostly K^+ and Ca^{2+}, influx through the opened mechanoelectrical transduction channels and depolarize the hair cell.

hereditary combined deaf-blindness in humans and is among the most common forms of recessive RP. It occurs in roughly 4 of every 100,000 individuals in developed countries such as United States (19, 94). Usher syndrome patients represent roughly one-sixth of all RP patients. Based on the different clinical courses of this disease, USH is further subdivided into three clinical types: USH1, USH2, and USH3. USH1 is the most severe form of this disease; USH1 patients display severe to profound congenital hearing impairments along with vestibular dysfunction and begin to lose their vision in childhood. USH2 is characterized by moderate to severe hearing impairments from birth onward, normal vestibular function, and the later onset of retinal degeneration. USH3 is distinguished from USH1 and USH2 by the later initiation of deafness and variable age of onset of retinal degeneration as well as vestibular dysfunction. Usher syndrome is inherited in an autosomal recessive manner, and different USH subtypes are genetically heterogeneous. So far, from genetic analysis of patient families, five (*MYO7A/USH1D*, *Harmonin/USH1C*, *CDH23/USH1D*, *PCDH15/USH1F*, *Sans/USH1G*) and three (*Usherin/USH2A*, *VLGR1b/USH2C*, and *Whirlin/USH2D*) genes have been identified to associate with USH1 and USH2, respectively, and one gene (*Clarin-1/USH3A*) has been linked to USH3 (4, 5, 8, 14, 17, 18, 28, 55, 64, 72, 81, 82, 88, 106, 107, 113, 114, 116, 117, 125). Mutations in these USH genes not only can cause syndromic disease but also may lead to nosyndromic hearing impairments (3, 6, 18, 49, 70, 78, 104). The detailed domain organizations of all identified USH proteins are summarized in FIGURE 2. Due to space limitations, this review mainly focuses on the USH1 proteins (namely myosin VIIa, harmonin, cadherin 23, protocadherin 15, and sans) and their specific functions in hair cells. Readers are referred to several excellent recent reviews on the functions of USH1 proteins in the visual system (32, 64, 91, 93, 119).

Properties of the USH1 Proteins

USH1B

MYO7A, the first identified USH gene (113), encodes myosin VIIa, an unconventional actin-based motor protein. From its NH_2 to COOH terminus, myosin VIIa can be divided into three main regions: the motor head domain, the neck region, and the tail cargo binding domains (FIGURE 2). The motor domain contains the actin-binding and ATP-binding sites and is responsible for the movement of the myosin along actin filaments. The neck region contains five IQ motifs, which are expected to bind to myosin-light chains such as calmodulin. The long-tail region starts with a single-helix domain (SAH), which serves as a lever-arm extension to enable large step sizes (61), followed by two MyTH4-FERM repeats separated by a SH3 domain. The myosin VIIa tail region binds to cargo proteins involved in endocytosis, cell-cell adhesion, and tip-link tension maintenance (26, 27, 42, 66, 102, 121), although a number of previously reported myosin VIIa binding proteins may be experimental artifacts due to inappropriate boundaries of the MyTH4-FERM protein used (see below for more details). It was also reported that the NH_2-terminal MyTH4-FERM tandem of *Dictyostelium* myosin VII binds to microtubules (75), which suggests a potential role of myosin VIIa in linking microtubule structures with actin filaments in specific regions of the cytoskeletons. Although myosin VIIa was originally thought to be a processive dimeric myosin (128), recent studies have shown that the purified full-length *Drosophila* myosin VIIa is a monomer rather than a dimer, and the tail domains can somehow inhibit the actin-activated ATPase activity of the motor domain (105, 127). Interestingly, its cargo molecules, such as MyRip/Rab27a, can induce myosin VIIa dimerization, thus activating it as a cargo transporter (95). The cargo binding-induced dimerization of myosin VIIa is analogous to that of myosin VI, another unconventional actin-based molecular motor (129). However, the detailed mechanisms governing the dimerization of myosin VIIa are still unknown. Myosin VIIa requires high ATP concentrations for its motor activity, since it has a much lower affinity for ATP than for ADP. It is a high-duty ratio motor, and ADP would greatly increase the binding affinity of myosin VIIa for actin filaments (45, 54). Therefore, myosin VIIa may also act as a molecular anchor to maintain tension in subcellular compartments that have high ADP concentrations. In mechanosensory hair cells, myosin VIIa is predominantly distributed in stereocilia but is also localized in the cuticular plates, along the lateral membrane, and in the synaptic regions (47, 48, 115). In stereocilia, myosin VIIa is coupled to the lateral and ankle links (71) and is concentrated at UTLD where it forms a tripartite complex with harmonin and sans (42). Studies on myosin VIIa-deficient mice indicate that myosin VIIa is essential for the development and organization of hair cell stereocilia (68, 96). Functional studies have further shown that myosin VIIa is responsible for maintaining tension by linking stereocilial membranes to the core structure formed by the actin filaments, thus creating tension in membrane-bound elements such as the tip links. Therefore, myosin VIIa is required for the normal gating of MET channels (65).

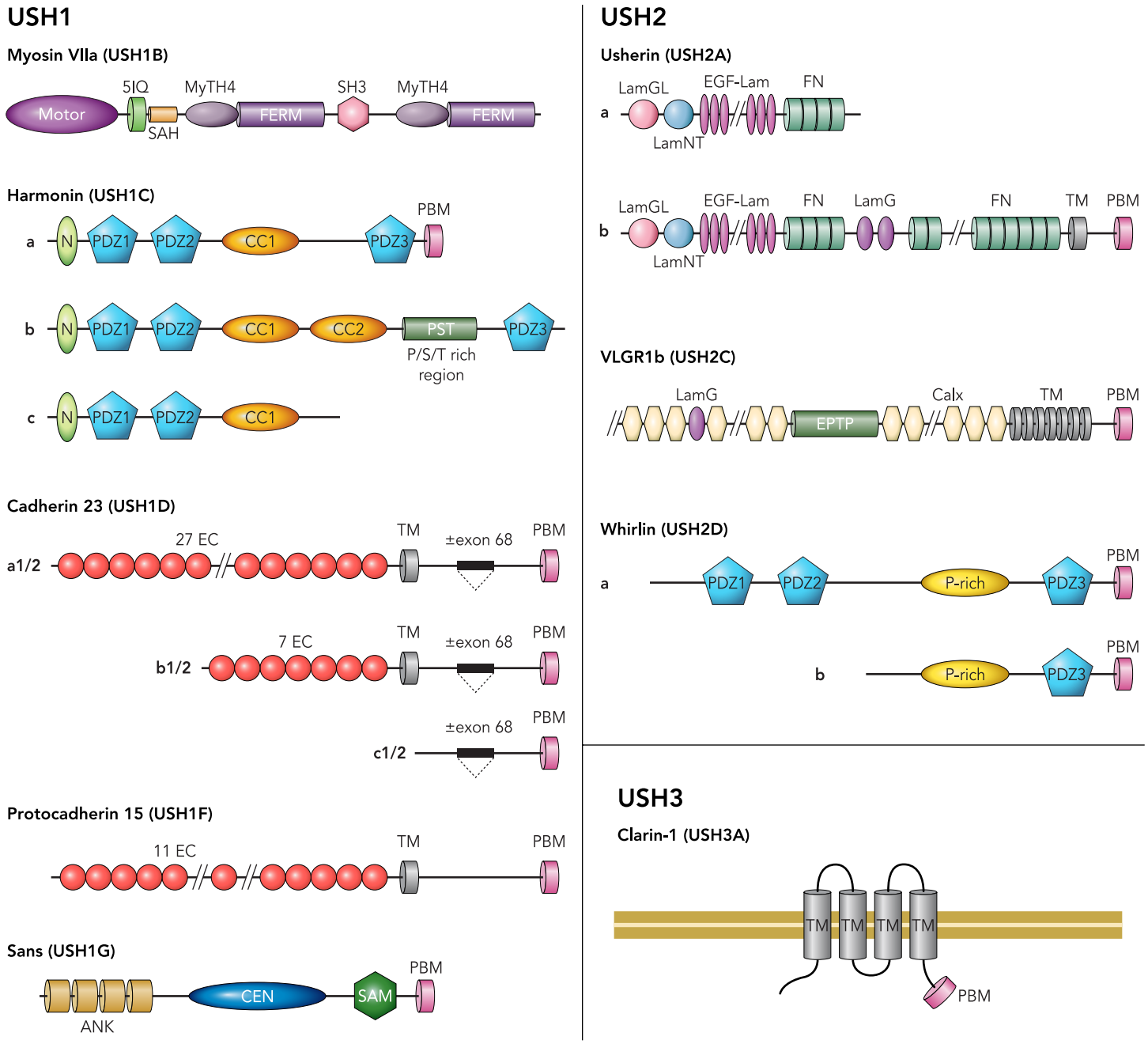

FIGURE 2. **Schematic drawing summarizing the domain organizations of the identified Usher syndrome proteins**
The USH1 proteins are drawn at *left*, and the USH2 and USH3 proteins are at *right*. The domain keys are shown at *bottom*.

USH1C

USH1C encodes harmonin, a PDZ domain-containing scaffold protein that was identified as the *USH1C* gene product first through the analysis of the USH1 mutations in several Acadian patients a decade ago (14, 107). Further genome screening and sequence analysis have revealed that the harmonin gene is not present in invertebrates, such as *Drosophila* or *C. elegans*, but is highly conserved in the genomes of vertebrates (89). Harmonins can be divided into three subclasses, namely a, b, and c (107). Each isoform contains a unique NH_2-terminal domain and two PDZ domains followed by one or two coiled-coil regions (FIGURE 2). Harmonin a and b both contain an additional PDZ domain at their COOH-terminal ends. Harmonin b also contains a PST (proline, serine, threonine-rich) region preceding the COOH-terminal PDZ domain, which functions together with the second coiled-coil region to bind to F-actin filaments and to induce filament bundling in vitro (15). Since PDZ domains are some of the most abundant protein-protein interaction modules in eukaryotic proteomes and play essential roles in the assembly of macromolecular protein complexes in diverse cellular processes (22, 130), the presence of three PDZ domains assigns harmonin as the key scaffold protein to organize the USH1 supramolecular protein complexes (1, 15, 90, 91). Analysis of harmonin transcription has revealed that the class b isoform is restricted largely to the inner ear, whereas the a and c isoforms have much broader expression profiles (107). In hair cells, harmonin b is detectable during cell differentiation and becomes concentrated at UTLDs of mature stereocilia (15, 44); the other harmonin isoforms localize along the stereocilia, in the cuticular plate, at the lateral plasma membrane, and at synapses throughout the life of mice (15, 43, 90). Studies of harmonin-deficient mice have revealed that harmonin b plays a role in coupling the activities of MET channels to the sound wave-induced stereocilia displacement and is essential for the proper stereocilia development (44, 56, 68).

USH1D

Mutations in the *CDH23* gene, which encodes for the cell adhesion protein cadherin 23, are responsible for USH1D (17, 18). Cadherin 23 is a calcium-dependent adhesion protein. Three subclasses of cadherin 23 isoforms, named a, b, and c, have been identified. Each subclass contains two sub-isoforms based on the presence or absence of exon68, which encodes for a unique insert in cytoplasmic tails (FIGURE 2). Therefore, alternative splicing generates at least six cadherin 23 isoforms: four transmembrane isoforms that are Ca^{2+}-mediated single transmembrane cell-cell adhesion molecules, which contain 27 (a1 and a2) or 7 (b1 and b2) extracellular cadherin repeats (ECs) followed by a single transmembrane helix and a short intracellular domain, and two cytosolic isoforms (c1 and c2) (67, 99). The extracellular ECs in classical cadherins (e.g., E- and N-cadherins) mediate the Ca^{2+}-dependent dimerization of cadherin molecules and the transcellular interactions between cadherin dimers of neighboring cells (98, 118). In contrast to classical cadherins, the cytoplasmic tail of cadherin 23 lacks the consensus R1 and R2-beta catenin binding sites (18), which are responsible for binding to the actin cytoskeleton (103). However, it contains a class I PDZ-binding motif (PBM) at the COOH terminus of its cytoplasmic tail, through which it can specifically bind to the PDZ2 domain of harmonin to anchor it to the actin cytoskeleton (1, 44, 99), although this has recently been refuted (131). The cadherin 23 (+68) splice isoform that contains exon68 is only expressed in the inner ear, whereas the cadherin 23 (−68) isoform is expressed in the kidney, heart, and spleen, as well as the brain and retina (15, 100). The function of this exon68 sequence is still largely unknown and a topic of debate (11, 99, 131). Our unpublished data shows that it can function as an internal motif to bind to the NH_2 terminal domain of harmonin, although we still do not know whether this in vitro interaction exists in in vivo setting or not. In mature hair cells, the full-length extracellular cadherin repeats of cadherin 23 form a Ca^{2+}-dependent homodimer and interact with protocadherin 15 in trans to form the tip links; in particular, cadherin 23 localizes at the upper part of tip link and contributes to the formation of UTLDs (57, 76, 100). In addition to the tip link localization, during the differentiation of hair cells, cadherin 23 is also localized at the transient lateral links and the kinocilial links, which are absent in mature hair cells (67, 73, 100). Cadherin 23-null mice show displacement of the kinocilia, fragmentation of hair bundles, and shortened stereocilia in hair cells, further demonstrating that cadherin 23 plays an important role in the hair bundle development and cohesion (23, 68, 120).

USH1F

The *PCDH15* gene product, protocadherin 15 (PCDH15), was identified as another Ca^{2+}-mediated single transmembrane cell-cell adhesion USH1 protein. It consists of 11 extracellular cadherin repeats, a single transmembrane motif, and a short intracellular domain with a class I PBM (FIGURE 2) (4, 8). PCDH15 also lacks the R1 and R2-beta catenin binding motifs in its cytoplasmic tail. Like cadherin 23, PCDH15 can also use its COOH-terminal class I PBM to specifically interact

with some PDZ domain-containing proteins, such as harmonin, to couple with the actin cytoskeleton (1, 87). In mature hair cells, PCDH15 is localized at the tips of the shorter rows of stereocilia. It uses its extracellular cadherin repeats to homodimerize and interact with cadherin 23 dimers to form tip links (57). So far, three prominent PCDH15 isoforms (PCDH15-CD1, PCDH15-CD2, PCDH15-CD3) have been identified; each contains a distinct cytoplasmic domain and a highly conserved extracellular region, and their spatiotemporal expression patterns in developing and mature hair cells differ (2). The CD1 isoform is expressed along the lengths of stereocilia; it is concentrated toward the bases and away from the tips. The CD2 isoform is distributed along the lengths of stereocilia during the development of hair cells but is absent from the stereocilia of mature hair cells. The CD3 isoform is concentrated at the tips of developing stereocilia and is expressed along the length of their shafts, but it becomes restricted to stereociliary tips as the hair bundle matures. Only the CD2 isoform is expressed in the kinocilium, and it is a component of kinocilial links (2, 40). The underlying mechanism governing the different spatiotemporal expression patterns of PCDH15 in hair bundles is still unknown, but it may involve molecules that interact with the unique PBMs or other motifs that differ across the three isoforms; for instance, harmonin and myosin VIIA have been shown to interact with the PCDH15-CD1 isoform in vitro (1, 97). The localization of PCDH15, especially its CD3 isoform, at LTLD and the fact that it acts as a component of the lower tip links suggests that it may directly or indirectly couple with the MET machinery and play a role in MET channel gating (38, 76). However, a recent study has shown that specific PCDH15-CD1 and PCDH15-CD3 knockout mice form normal hair bundles and tip links and maintain normal hearing function. Only PCDH15-CD2-deficient mice are deaf and have abnormally polarized hair bundles due to the lack of kinociliary links (111). Interestingly, tip links are still present in the PCDH15-CD2-deficient mice. Thus it seems that the PCDH15 isoforms can function partially redundantly in hair cells, in particular for the tip link formation (111). The severe defects of stereocilia development and profound deafness of Ames waltzer mice, which bear mutations in all PCDH15 isoforms, clearly indicate that PCDH15 plays important roles in the morphogenesis as well as the maintenance of the stereocilia in hair cells (7, 46, 68).

USH1G

The scaffold protein sans was first identified as the gene product underlying *USH1G* by genetic mapping of two consanguineous USH1G-affected families in 2003 (114). Sans consists of several putative protein-protein interaction modules: four NH_2-terminal ankyrin repeats (our laboratory's unpublished data), a central region followed by a sterile alpha motif (SAM), and an extreme COOH-terminal class I PBM (FIGURE 2) (69, 86, 130). Although ankyrin repeats have been reported to mediate protein-protein interactions in other proteins, the binding partners for sans ankyrin repeats are still unknown. The central domain interacts with myosin VIIa's two MyTH4-FERM tail domains (1, 122). The SAM domain and the COOH-terminal PBM can both bind to the PDZ1 domain (or rather the N-PDZ1 domains) of harmonin (114, 126). The expression of sans is found in the inner ear, eye, and small intestine (114). During hair cell differentiation, sans is localized in the apical regions of hair bundles and is present at the hair bundle tips, where it is required for the cohesion of hair bundles of hair cells during their early development (20). In mature hair cells, sans is observed in the apical regions of all three rows of stereocilia and is concentrated at UTLDs (20, 42, 124). In sans-deficient mice, the cohesion of stereocilia is disrupted, and both the amplitude and the sensitivity of transduction currents are reduced, suggesting that sans is required for the proper function of the MET machinery, especially for the maintenance and renewal of tip links (20, 59, 68).

The USH1 Protein Complexes

Molecular studies have shown that all of the five USH1 proteins can interact with at least one other USH1 protein, forming a network that has been referred to as the USH1 interactome (FIGURE 3) (1, 15, 24, 57, 64, 74, 88, 90, 92, 97). Harmonin and sans function as the master scaffolds in the assembly of the USH1 protein network, since harmonin is capable of directly binding to all of the other USH1 proteins through its PDZ domains (1, 15, 91, 99, 114) and sans can further bind to myosin VIIa through its central region (1, 122). In addition, cadherin 23 and PCDH15 interact with each other in trans to form tip links via their extracellular cadherin repeats (57). Consistent with this in vitro biochemical interaction network, mice containing mutations of any one of the USH1 proteins display common morphological defects in the stereocilia of hair cells (7, 20, 23, 56, 59, 68, 96, 110). These genetic studies also indicate that the assembly of the USH1 interactome is essential for the coordinated differentiation of stereocilia during hair cell development and the maintenance of mechano-electrical signal transductions in mature hair cells (24, 38, 42, 64, 76, 88). Besides this, the presence of many USH1 proteins in the synaptic regions of hair cells suggests that the USH1 interactome may also

play a role in the synaptic transmissions of sound signals (88, 90). Systematic biochemical and structural investigations in the last few years have provided an unprecedented clear picture of the USH1 protein complex organization and have explained at the atomic level why mutations found in these *USH1* genes can lead to hearing deficits in humans.

Atomic Pictures of the USH1 Protein Complexes

Structural Insight into the Cadherin 23/PCDH15 Interaction

Tip links are formed by cadherin 23 homodimers, which interact in trans with PCDH15 homodimers to form extended filaments (57). The ectodomains of cadherin 23 and PCDH15 are characterized by repeating amino acid sequences of ~110 residues, each of which corresponds to a Greek-key topological protein module called the "extracellular cadherin" (EC) domain. Each classical EC domain is composed of seven β-strands forming a β-sandwich fold with the amino and carboxyl termini at the opposite ends; multiple ECs further assemble into a rigid EC-strand through Ca^{2+}-coordinated inter-EC linkers (85). Previous studies of classical cadherins have revealed that the adhesive trans-cadherin binding site is mainly localized at the respective membrane-distal EC1 domain of two cadherins. A domain-swapping interaction between two juxtaposed EC1 domains of two cadherins from two opposing membrane leaflets represents the general mechanism for the in trans homophilic adhesions found in the type I and type II cadherins (16, 80) (FIGURE 4, B AND C). In the

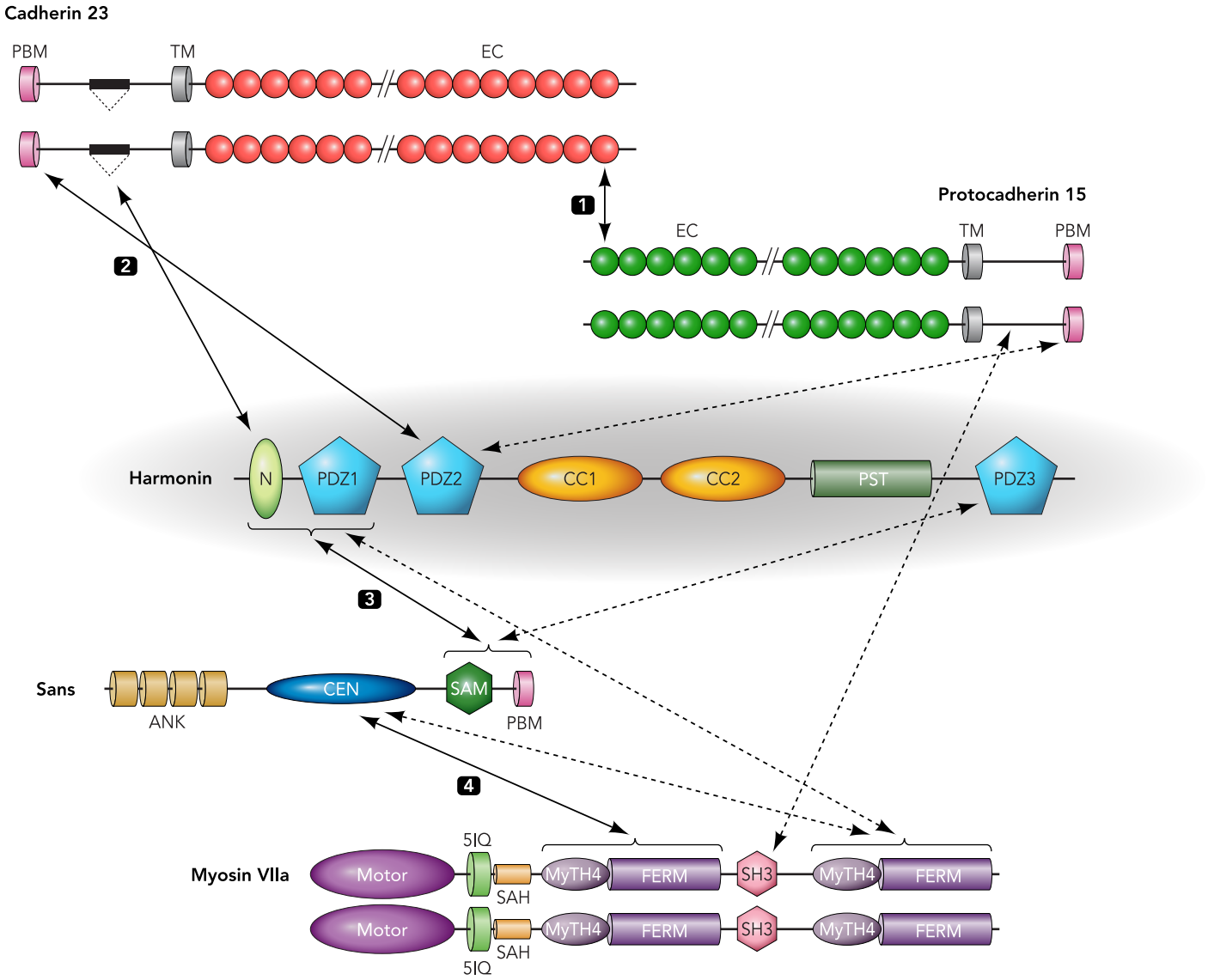

FIGURE 3. **The USH1 protein interaction network**
In this presentation, the interactions that have been characterized by detailed structural studies and are summarized in this review are indicated with the solid arrows and further labeled with roman numbers. The interactions that were previously reported but lacking detailed structural information are indicated with the dashed arrows. The figure also highlights that harmonin is capable of functioning as the organization center for the assembly of the USH1 interactome.

type I homophilic cadherin interaction, a short NH_2-terminal fragment containing the highly conserved Trp2 of one EC1 domain crosses over to the neighboring EC1, forming a domain-swapped EC1 homodimer in which the bulky side chain of Trp2 inserts into the hydrophobic pocket of the neighboring EC1 (FIGURE 4B). In the type II cadherin interaction, two conserved Trp residues (Trp2 and Trp4) in the domain-swapped NH_2-terminal fragment of EC1 play critical roles in the formation of the EC1 homodimer (FIGURE 4C). Interestingly, amino acid sequence analysis indicates that both cadherin 23 and PCDH15 lack the signature hydrophobic Trp residue(s) in the NH_2-termini of their respective EC1 domains, implying that the heterophilic cadherin 23 EC1/PCDH15 EC1 interaction may follow a mode that is different from those seen in the classical cadherins. Recently, the high-resolution structure of the EC1–2 domains of cadherin 23 have shown that both EC1 and EC2 adopt the characteristic cadherin domain fold and that the two domains couple with each other using three conserved Ca^{2+}-binding motifs at their linker regions (25, 101). Interestingly, the EC1–2 domains of cadherin 23 form monomers, and the elongated NH_2-terminal extension of EC1 contains a small α-helix followed by a short β-strand. Asn3 and Arg4 of the EC1 extension, together with the β2/β3- and β6/β7-loops of EC1, form a rather unique Ca^{2+}-binding site at the distal end of EC1, and residues from the small α-helix and the short β-strand of the NH_2-terminal extension insert into the hydrophobic pocket of EC1 (FIGURE 4A), which in classical cadherins is occupied by the Trp residue(s) from the domain-swapped NH_2-terminus (FIGURE 4, B AND C). Since mutations of Asn3 and Arg4 in the NH_2-terminal extension abolish the interaction between cadherin 23 and PCDH15 (25), it is possible that the unique intramolecular interaction between the NH_2-terminal extension and the EC1 core of cadherin 23 creates a binding surface for PCDH15 EC1. We note with interest that the corresponding NH_2-terminal extension of PCDH15 EC1 is also essential for the cadherin 23/PCDH15 interaction (25). Alternatively, it is also possible that the NH_2-terminal extension of cadherin 23 EC1 may interact with the PCDH15 EC1 via a domain-swapping mechanism similar to that observed in the classical cadherins shown in FIGURE 4, B and C. However, unlike homodimers of the classical cadherins, which align in trans by contacts mainly formed between the two opposing

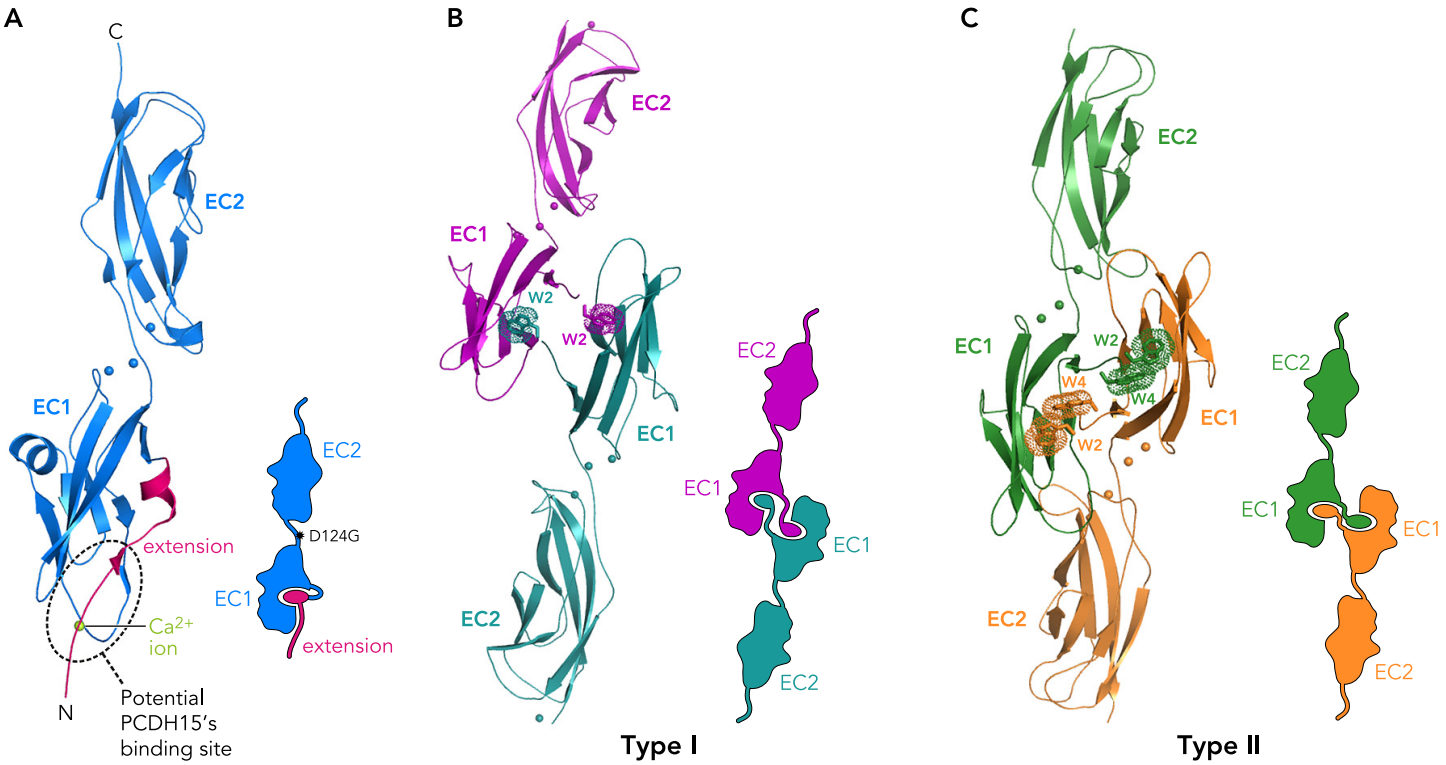

FIGURE 4. **The structure and possible interacting mode of the EC1–2 tandem of cadherin 23**
A: ribbon diagram representation showing the overall structure of the EC1–2 tandem of cadherin 23 (PDB access code 2WHV). In this diagram, the unique NH_2-terminal extension of cadherin 23 is colored in pink, and the EC1–2 tandem is in blue. The NH_2-terminal-bounded Ca^{2+} ion as well as the potential PCDH15 binding site are further highlighted and labeled. The schematic diagram at the *bottom right* shows the domain organization of the EC1 and EC2 as well as the interaction of the NH_2-terminal extension with EC1. The position of the D124G missense mutation from human patients is further indicated and labeled (also see Table 1). *B* and *C*: the combined ribbon and stick-dot representations show hemophilic cadherin-mediated adhesions. *B* and *C* depict the classical type I (PDB access code 1L3W) and II (PDB access code 1ZVN) EC1-mediated dimerization models of cadherins. It is noted that EC1 is assembled into homodimers via swapping a short, Trp-containing NH_2-terminal fragment between the two subunits in both types of the hemophilic interactions.

EC1 domains, two cadherin 23 and two PCDH15 molecules in tip links may align with each other via larger parts of their extracellular domains to form more extensively intertwined dimers-of-dimers (57). Such dimer-of-dimer cadherin 23/PCDH15 assembly may allow tip links to sustain a substantially larger range of mechanical forces during stimulations of hair cells (84). It is clear that more structural work is needed to understand how the EC domains of cadherin 23 and PCDH15 interact with each other in trans to construct the tip link connections between stereocilia.

The Multidentate Interactions between Harmonin and Cadherin 23

Tip link filaments can consistently withstand large forces (>100 pN) under stimulated conditions (84), whereas forces of 10–20 pN can pull most single-path transmembrane proteins out of membrane leaflets (12). The cytoplasmic tail of cadherin 23 likely plays important roles in anchoring tip links to UTLD to assure that the link will not be pulled out under large mechanical forces. The cytoplasmic tail of cadherin 23 contains a type I PBM, which can specifically bind to the PDZ2 domain of harmonin (15) as well as the PDZ4 domain of MAGI-1 in vitro (123). In addition, it harbors an internal motif that has been reported to interact with an NH_2-terminal fragment of harmonin from the start of the NH_2-terminus to the PDZ1 domain (99). Our recent structural study has revealed that a highly conserved ~80-residue fragment preceding the PDZ1 domain of harmonin (referred to as the N-domain) adopts an autonomously folded structure that contains five α-helices and forms a novel five-helix-bundle fold (79) (FIGURE 5A). Earlier biochemical studies missed the role of harmonin N-domain and mistakenly assigned all N-PDZ1's functions to the PDZ1 domain. Our biochemical and structural studies revealed that the harmonin N-domain directly binds to a short peptide fragment within the cytoplasmic tail of cadherin 23 (referred to as NBM in FIGURE 5, A AND B) using a solvent-exposed, V-shaped hydrophobic cleft formed by the αA/αB helix-hairpin of the domain (11, 79, 131) (FIGURE 5, A AND B). Thus the interaction between the cadherin 23 tail and harmonin is mediated by this N-domain, rather than by the PDZ1 domain as previously assumed. Our laboratory's unpublished findings further reveal that a small fragment encoded by exon68 (referred to as EXON68 in FIGURE 5, A AND C) of cadherin 23 can also specifically bind to the N-domain of harmonin. The molecular mechanism governing the interaction between the harmonin N-domain and the cytoplasmic tail fragments (NBM and EXON68) of cadherin 23 was elucidated by solving the structures of the N-domain in complex with both the NBM peptide and the EXON68 peptide, respectively (FIGURE 5, B AND C). The complex structures reveal that NBM and EXON68 bind to N-domain via highly similar mechanisms, each forming an amphipathic α-helix and binding to the exposed hydrophobic pocket formed by the αA/αB helix-hairpin (FIGURE 5, B AND C). In addition to the N-domain and the internal peptide fragment interactions described above, the interaction between harmonin and cadherin 23, at least in vitro, also involves harmonin PDZ2 and the PBM of cadherin 23. The structure of harmonin PDZ2 in complex with the PBM of cadherin 23 demonstrates that harmonin PDZ2 adopts a canonical PDZ domain fold with an additional short α-helix following the final βF strand. The cadherin 23 PBM binds to the αB/βB-groove of PDZ2 by augmenting the βB-strand of the PDZ2 domain in an anti-parallel manner (FIGURE 5D). Therefore, the formation of the harmonin/cadherin 23 complex can occur via a multidentate interaction between the two proteins (FIGURE 5E), and this interaction mode is presumably thermodynamically favorable for the stability of the cadherin 23/harmonin complex at UTLD. The dimerization of cadherin 23 would further increase the avidity of the interaction between the two proteins (FIGURE 5E). It has been reported that the COOH-terminal "PST"-domain of harmonin b may function as an anchor to couple the tip link complexes to the actin cytoskeleton (15, 44). Thus it is envisioned that the actin filament-attached cadherin 23/harmonin complex, which may be further cross linked to actin filaments by the myosin VIIA/sans complex (see below for details), is highly stable and forms part of the UTLD protein complex in stereocilia (FIGURE 5F). Consistent with these structural findings, a recent functional study has shown that the harmonin/cadherin 23 and harmonin/F-actin interactions control harmonin localization in stereocilia and are necessary for normal hearing (44). The study reveals that the interaction between harmonin PDZ2 and cadherin 23 PBM plays a critical role in clustering cadherin 23 in UTLD of stereocilia (44). It is likely that the multidentate interaction between harmonin and cadherin 23 plays an important role in the assembly of stable tip link complex formed by cadherin 23/PCDH15 in hair cells. It should be noted that two recent in vitro studies have also shown that the harmonin/cadherin 23 complex is primarily mediated by the interaction between harmonin N-domain and cadherin 23 NBM. Deletion of either EXON68 or PBM of cadherin 23 has no obvious effect on the interaction between harmonin and cadherin 23 based on their used assay methods (11, 131). These findings argue against the potential roles of the PBM and EXON68 of cadherin 23 in

binding to harmonin in hair cells, but further work is required to confirm these findings.

The Harmonin/Sans Interaction

In addition to binding to cadherin 23 through its N and PDZ2 domains, harmonin also has been reported to associate with sans (1, 114), and the two proteins are co-localized at UTLD of hair cells (42). In sans-deficient Jackson mice, harmonin is completely absent in hair cells from the embryonic stage onward (68), implying that sans is required for the trafficking of harmonin to stereocilia. In an earlier study, the interaction between harmonin and sans was mapped to the PDZ1 and PDZ3 domains of harmonin and the SAM domain, including the COOH-terminal PBM (SAM-PBM), of sans. Interestingly, both the SAM domain and PBM of sans can specifically bind to the PDZ1 domain of harmonin (1). However, the interaction between harmonin PDZ3 domain and sans could not be detected in our hands (our laboratory's unpublished data). Since the SAM domain is known to be a protein-protein interaction

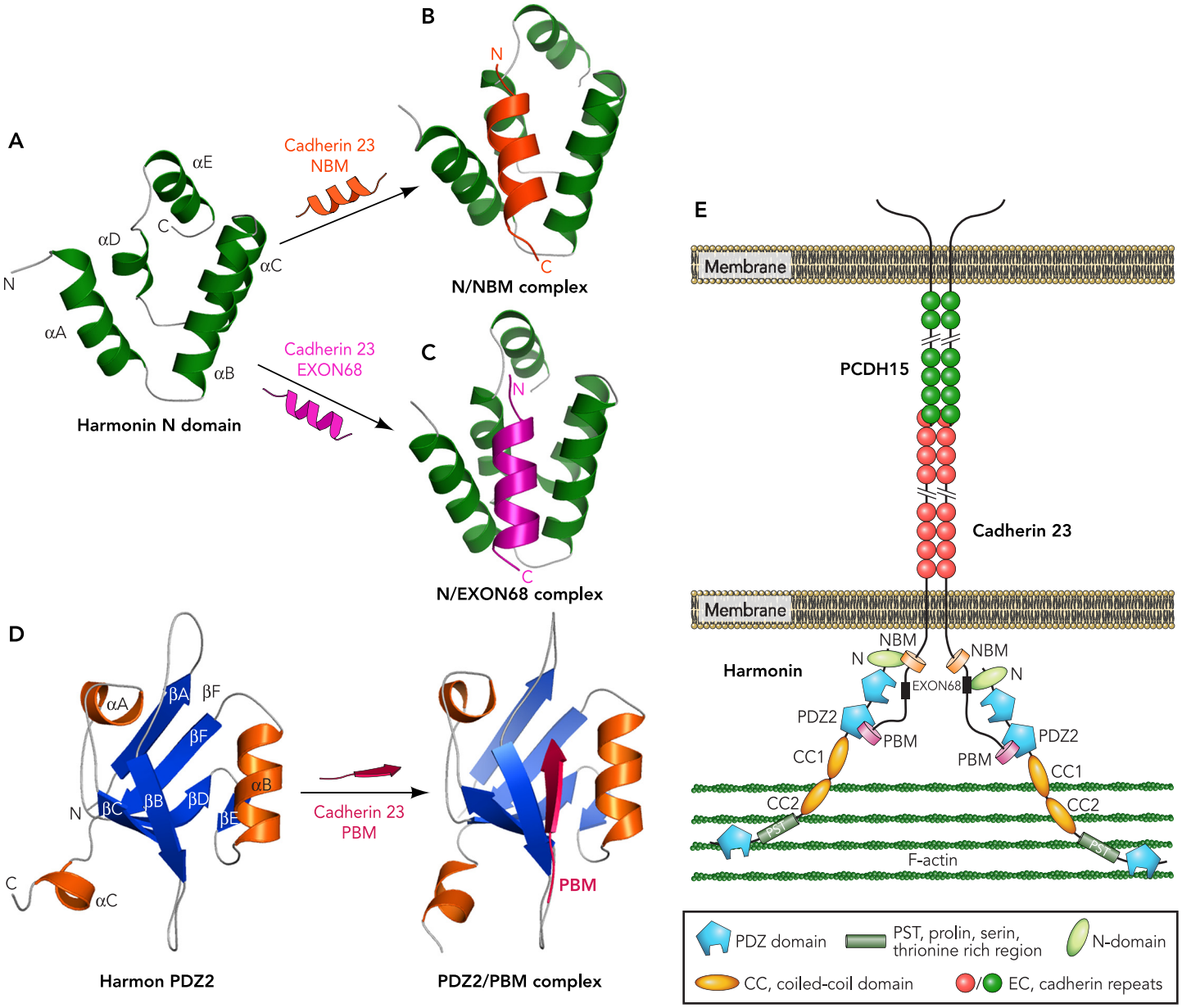

FIGURE 5. **The multidentate interactions between harmonin and cadherin 23**
A–C: ribbon diagram representations of the apo-harmonin N-domain (*A*; PDB access code 2KBQ), the structure of the N-domain/NBM peptide complex (*B*; PDB access code 2KBR), and the structure of the N-domain/EXON68 peptide complex (*C*; our laboratory's unpublished result). *D*: specific interaction between harmonin PDZ2 and the cadherin 23 PBM revealed by the structure of the PDZ2/PBM complex (PDB access codes 1X5N and 2KBS). *E*: a schematic cartoon diagram depicting a model of the multidentate interaction between harmonin and dimerized cadherin 23 at the tip link of hair cells. In this model, harmonin, via its N-domain and PDZ2, interacts with an internal peptide fragment (either PBM or EXON68) and the COOH-terminal PBM of the cytoplasmic tail of cadherin 23, respectively. This multidentate interaction between harmonin and cadherin 23, together with the dimerization of cadherin 23, is thought to enhance both specificity and stability of the assembly of the tip link complex in hair cells. Harmonin can further connect the tip link complex to the actin cytoskeleton via its PST module.

module capable of forming homo- and hetero-oligomers (86), the formation of a SAM/PDZ complex is highly unusual given our understanding of the canonical target-binding modes of both SAM and PDZ domains (86, 130). The high-resolution structure of harmonin NPDZ1 in complex with sans SAM-PBM explains this highly unusual interaction mode (126). The SAM domain of sans adopts the canonical five-helix SAM domain fold. Together with its PBM, the sans SAM domain forms a highly stable complex with harmonin NPDZ1 (FIGURE 6A). In this complex, the SAM domain makes extensive contact with harmonin PDZ1 through an interaction mode that is novel for both SAM and PDZ domains, and the sans PBM concomitantly binds to harmonin PDZ1 via the canonical PDZ/target interaction mode (FIGURE 6, A AND C). The synergistic SAM/PDZ1 and PBM/PDZ1 interactions between sans and harmonin lock the two scaffold proteins into a highly stable complex (a dissociation constant of ~2 nM). Interestingly, the complex structure also reveals that harmonin NPDZ1 forms a structural supramodule with its N-domain and PDZ1 integrated by a mini-domain formed by a conserved COOH-terminal extension, which is composed of a small β-hairpin followed by a short α-helix (FIGURE 6B). The structure of the NPDZ1 supramodule represents the first example of a PDZ domain that intimately packs with another unrelated protein-protein interaction domain to form a heterotypic supramodule and reveals a novel tandem-domain assembly mode involving PDZ domains (29, 126).

In the harmonin NPDZ1/sans SAM-PBM complex, the conformation of the N-domain is essentially the same as that of the isolated domain,

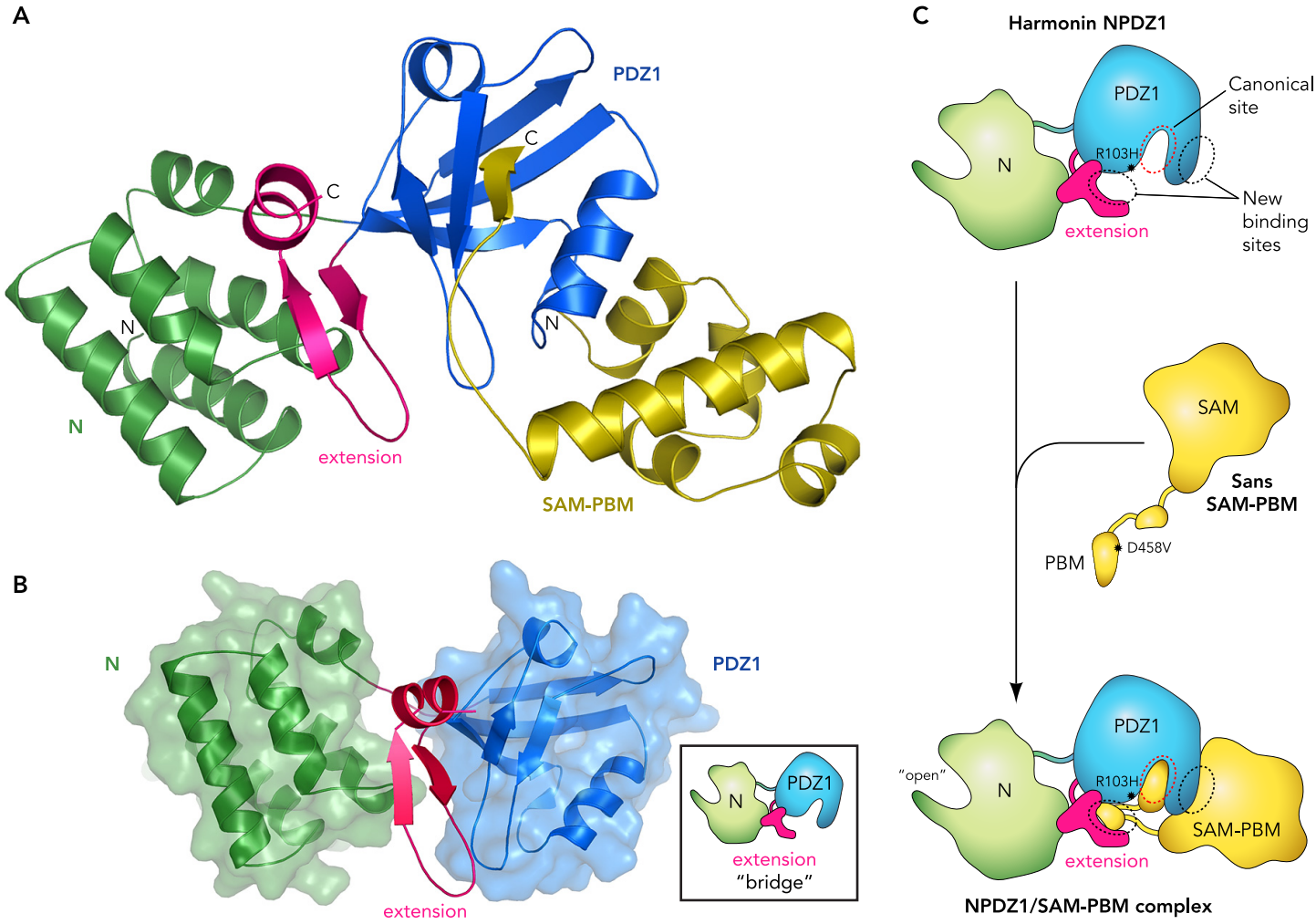

FIGURE 6. **The interaction between harmonin and sans**
A: ribbon diagram showing the overall structure of the harmonin NPDZ1/sans SAM-PBM complex (PDB access code 3K1R). In this drawing, the N-domain is shown in green, PDZ1 domain in blue, mini domain in pink, and SAM-PBM in olive. *B*: surface representation showing the domain architecture of harmonin NPDZ1 supramodule with the same color scheme as in *A*. *C*: a schematic cartoon diagram summarizing the interaction between harmonin NPDZ1 and sans SAM-PBM. The identified disease-associated R103H missense mutation of harmonin and D458V of sans are further indicated and labeled at *top* (also see Table 1). The NPDZ1 supramodule contains three distinct target binding sites for sans SAM-PBM, which are a canonical PDZ-motif binding pocket, a novel SAM domain-interacting site, and an accessary site formed by the PDZ1 and mini-extension domain interface.

and the target-binding cleft formed by the αA/αB helix-hairpin is located at the opposite side of the SAM/PDZ1 interface and hence is fully exposed (FIGURE 6, A AND C), indicating that the N-domain in the harmonin/sans complex is still capable of binding to cadherin 23. Therefore, the tightly assembled harmonin/sans complex can serve as the nucleation core for the entire USH1 interactome. Additionally, this complex can further interact with other unidentified partners to form even

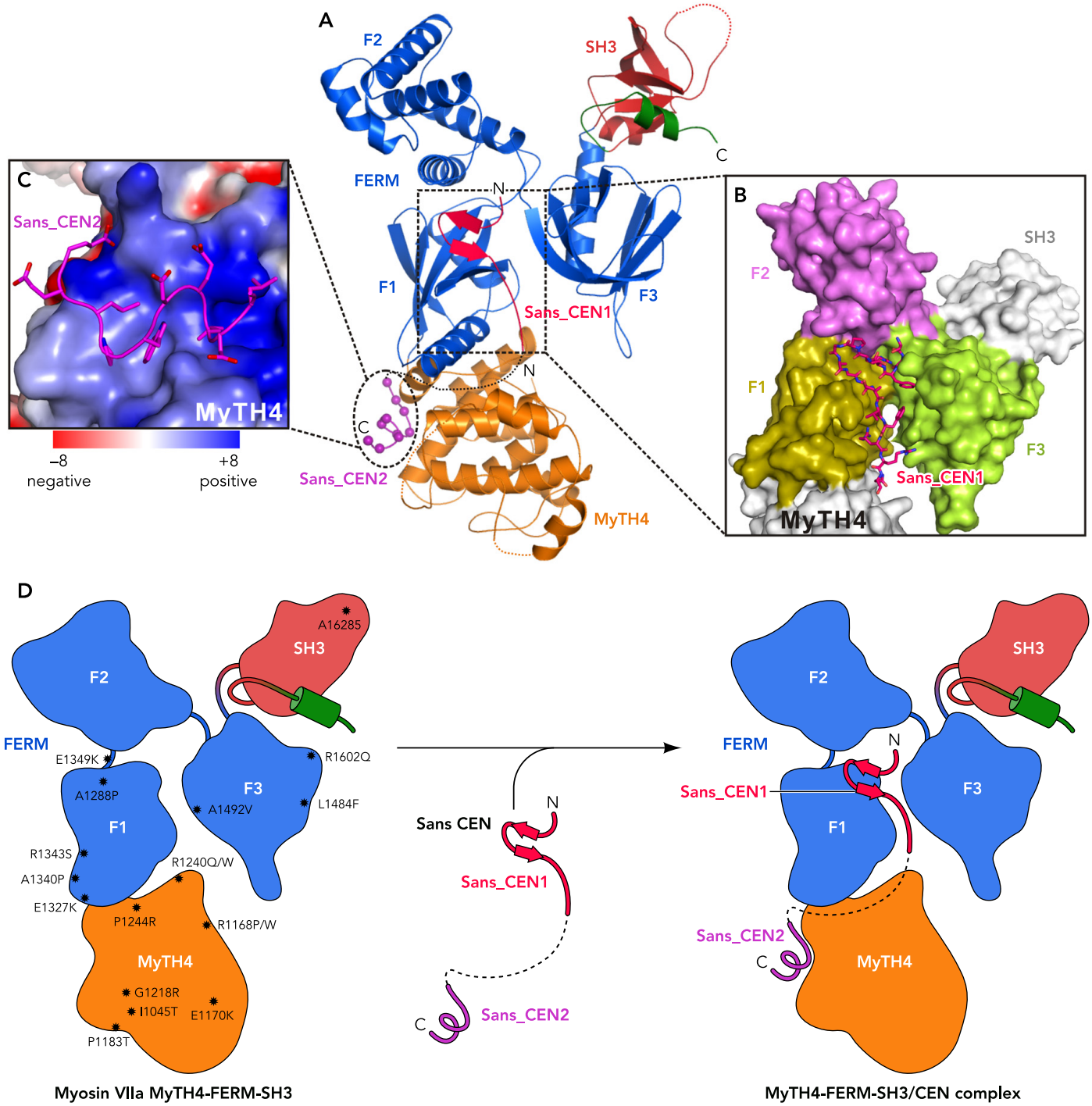

FIGURE 7. **Structural basis of the myosin VIIa MFS and sans interaction**
A: ribbon diagram representation of the overall structure of the myosin VIIa MFS/sans CEN complex (PDB access codes 2L7T and 3PVL). Two disorder regions in the MyTH4 domain and one in the SH3 domain are indicated by the dotted lines. *B*: the surface representation showing the binding interface between the FERM domain of the myosin VIIa MFS and sans CEN1. The F1, F2, and F3 lobes of FERM are in direct contact with sans CEN1, which is shown in explicit atomic model. *C*: surface representation showing the detailed binding interface between the CEN2 peptide and the MyTH4 domain. The figure shows that the charge properties of MyTH4 and CEN2 are highly complementary. *D*: a schematic cartoon diagram summarizing the overall interaction mode between myosin VIIa MFS and sans CEN. The identified missense mutations in myosin VIIa MFS from human patients are further indicated and labeled at *left* (also see Table 1).

larger macromolecular complexes through their unoccupied protein-protein interaction modules, such as the NH_2-terminal four ankyrin repeats of sans and the COOH-terminal PDZ3 domain of harmonin.

Structural Basis of the Myosin VIIa/Sans Interaction

Another important question in hair cell development is how harmonin and sans are transported to and anchored at UTLD of stereocilia. Since stereocilia are filled with polarized actin filaments, the actin-based unconventional myosin VIIa motor likely plays critical roles in the cellular localization of harmonin and sans. Genetic studies have shown that the targeting of harmonin-b to the stereocilia tips depends on both myosin VIIa and sans (68), and biochemical analysis has shown that myosin VIIa can directly bind to both harmonin (15) and sans in a mutually exclusive manner (1). However, we could not detect any direct interaction between myosin VIIa and harmonin (our laboratory's unpublished data). Instead, we believe that myosin VIIa and harmonin associate with each other using sans as the bridging protein (122). This biochemical finding is consistent with recent cell biology data showing that myosin VIIa, sans, and harmonin are co-localized at UTLD of stereocilia in mature mouse hair cells (42). The specific interaction between myosin VIIa and sans is mainly mediated by the central region (referred to as CEN) of sans and the tail region of myosin VIIa. Both MyTH4-FERM tandems in myosin VIIa tail have been reported to interact with the CEN region of sans (1), although the involvement of the COOH-terminal MyTH4-FERM in sans binding is not yet well substantiated. The recently solved structure of myosin VIIa MyTH4-FERM-SH3 (MFS) in complex with the CEN domain of sans from our laboratory not only provides the first portrait of a MyTH4-FERM tandem at the atomic level but also reveals a unique cargo recognition mode for the MyTH4-FERM tandem in myosin motors in general (122) (FIGURE 7). In the myosin VIIa MFS/sans CEN complex, the myosin VIIa MFS adopts an overall Y-shaped architecture comprising three domains: the NH_2-terminal MyTH4 domain, the middle FERM domain that is composed of F1, F2, and F3 lobes forming a cloverleaf-like structure, and the COOH-terminal SH3 domain (FIGURE 7A). The MyTH4 domain adopts a novel 10-helix bundle architecture and makes direct contact with the FERM F1 lobe. The residues that are critical for the inter-MyTH4/FERM interface interactions are absolutely conserved in the myosin VIIa MyTH4-FERM tandems as well as in all other MyTH4-FERM

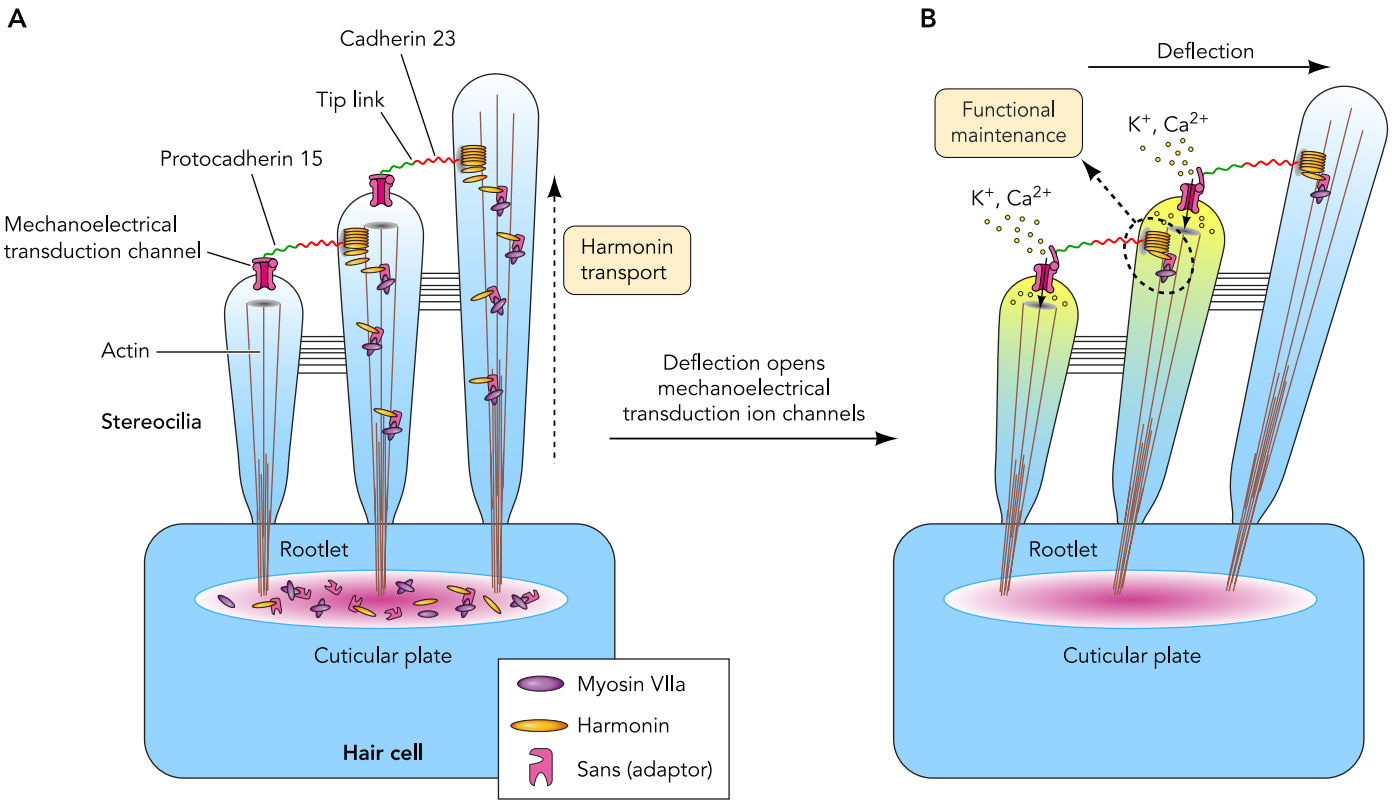

FIGURE 8. **Possible functional models for the myosin VIIa/sans/harmonin tripartite complex in the stereocilia of hair cells** *A*: a schematic diagram depicting a possible model showing the myosin VIIa-mediated intra-stereocilia transport of harmonin and harmonin-bound Usher proteins in stereocilia of hair cells. In this model, sans functions as an adaptor to bridge harmonin to the actin-based myosin VIIa motor. *B*: another schematic model showing that myosin VIIa, sans, and harmonin co-cluster at UTLD and form a tripartite complex for possible maintenance of the MET channel function in mature hair cells.

Table 1. A partial list of disease-associated missense mutations of the USH1 proteins that can be rationalized by the currently available structures

	Proteins	Identified Missense Point Mutations	Structural Explanations
USH1B	Myosin VIIa	I1045T, R1168P/W, E1170K, P1183T, R1240Q/W, P1244R, A1288P, L1484F, E1812K/R, L1836P, L1858P	Disrupt the folding of MyTH4 or FERM domain
		E1327K, A1340P, R1873W/Q, R1883Q, P1887L	Disrupt or interfere with the MyTH4/FERM interaction interface
		G1218K, E1349K, A1492V	Disrupt or interfere with the myosin VIIa/sans binding interface
		R1343S, R1602Q, A1628S	Disrupt or interfere with myosin VIIa/potential new targets interface
USH1C	Harmonin	R103H	Interfere with the harmonin/sans binding interface
USH1D	Cadherin 23	D124G	Interfere with the EC/EC interaction interface
USH1F	PCDH15	Q1342K	Disrupt or interfere with PCDH15/potential new targets interface*
USH1G	Sans	L48P	Disrupt the folding of ankyrin repeats*
		D458V	Interfere with the sans/harmonin binding interface

*Our laboratory's unpublished structural data.

tandem-containing proteins (50, 112, 122), indicating that MyTH4 and FERM domains connected in tandem always form integral structural and functional supramodules. Indeed, the MyTH4-FERM tandem of myosin VIIa forms a structural supramodule capable of binding to two highly conserved segments (CEN1 and CEN2) of the sans central domain (FIGURE 7, A AND D). The CEN1 segment in the MFS/CEN complex adopts a short NH_2-terminal β-hairpin and a COOH-terminal extended structure and binds to the central interface formed by the F1, F2, and F3 lobes of the FERM domain (FIGURE 7B); this interaction contributes to the majority of the binding energy between myosin VIIa and sans. The interaction between myosin VIIa FERM and sans CEN1 represents a novel recognition mode for FERM domains. In all other FERM/target interactions, the contact sites between a FERM domain and its targets occur at the surfaces of one or at most two lobes of the domain located at the outer faces of the three "leaves" of the clover formed by the three lobes. In contrast, sans CEN1 binds to the center of the clover using the interfaces formed by the inner faces of the three FERM lobes (FIGURE 7B). The interaction between myosin VIIa MyTH4 and sans CEN2 is much weaker but nonetheless critical for establishing binding specificity between myosin VIIa MFS and sans CEN (122). NMR spectroscopy-based studies have shown that the negatively charged CEN2 adopts a defined extended conformation and specifically binds to a highly positively charged pocket on the MyTH4 domain (FIGURE 7C). The myosin VIIa MFS/sans CEN complex also provides direct evidence showing that MyTH4 domains in a number of unconventional myosins, including myosin VIIa, are likely to function as protein binding modules. It is also worth mentioning that the integration of MyTH4 and FERM domains into a structural and functional supramodule explains the observation that MyTH4 domains invariably co-exist with FERM domains in all known MyTH4 domain-containing proteins and provides a structural guideline for studying MyTH4-FERM domain proteins in the future. It should be noted that the majority of the MyTH4-FERM domain studies reported in the literature, either in attempts to map target binding region or to locate the functional subdomains within the tandem, involved inappropriate selections of domain boundaries or the physical separations of the MyTH4 and FERM domains. Therefore, caution should be exercised in interpreting the results from such studies.

Furthermore, the MFS/CEN complex structure, together with the complex structure of sans SAM-PBM and harmonin NPDZ1, immediately suggests that there should be no competition between harmonin and myosin VIIa in binding to sans. Instead, sans is ideally suited to function as an adaptor for the formation of the myosin VIIa/sans/harmonin tripartite complex. The formation of the myosin VIIa/sans/harmonin tripartite complex provides a mechanistic explanation for the myosin VIIa-mediated transport of harmonin from the cuticular plates to UTLD of stereocilia during hair cell development (FIGURE 8A). Additionally, since harmonin may multimerize via its central coiled-coil domains, the myosin VIIa/sans/harmonin tripartite complex can further form high-density, actin filament-coupled clusters at UTLD in mature hair cells (FIGURE 8B). Via the harmonin/cadherin 23 connection at UTLD (FIGURE 5), myosin VIIa may exert mechanical forces to generate tension on tip links (42). Therefore, it is possible that the myosin VIIa/sans/harmonin tripartite complex may play different roles during the development of hair

cells and in the maintenance of mature hair cells function. Further work is required to verify and dissect these two possibilities.

Mechanistic Explanations of Disease-Associated Mutations in USH1 Proteins

A fundamental question in Usher syndrome studies is to understand why mutations in the *USH1* genes can cause diseases. As discussed above, structural studies of USH1 proteins cannot only provide mechanistic insight into the organization of the USH1 protein complexes and the physiological functions of the USH1 proteins in normal development and functions of hair cells but can also help to explain the molecular bases of many disease-associated mutations in these proteins. The deleterious effects of many missense mutations found in Usher syndrome patients can be clearly explained based on the high-resolution structures of the USH1 proteins and their complexes determined in recent years (summarized in Table 1). For example, the MyTH4-FERM/sans complex structure provides clear mechanistic explanations for the 19 disease-causing missense mutations identified in the MyTH4-FERM region of myosin VIIa in USH1 patients (122) (FIGURE 7D and Table 1). The structure of the harmonin NPDZ1/sans SAM-PBM complex also reveals that two missense mutations found in harmonin and sans, R103H in harmonin and D458V in sans, lead to destabilization of the harmonin/sans complex (126).

Concluding Remarks

Human genetic studies and the use of animal models have allowed us to identify and explore the functions of a wide list of proteins that are critical for the development of stereociliary bundles and the proper function of mature hair cells. Biochemical studies have revealed that the five USH1 proteins can interact with each other to form an integral protein-protein interaction network. The recently solved atomic structures of a number of USH1 protein complexes have shed light on the mechanistic basis of how the five USH1 proteins function together in controlling the proper development as well as physiological functions of hair cells. These mechanistic insights include how cadherin 23 and PCDH15 interact with each other to construct stereociliary tip links; how harmonin and cadherins together form high-density stable bases in anchoring tip link cadherins on to the stereocilia; how myosin VIIa delivers its cargoes such as harmonin from the hair cell body to stereocilia tips with the help of the adaptor protein sans; and how myosin VIIa may function as a connecting molecule in linking the cadherin 23/harmonin/sans complex at UTLD with the actin filaments within the stereocilia. In addition, these USH1 complex structures can provide valuable mechanistic explanations of hearing deficiencies caused by mutations in these proteins. Finally, detailed structural studies of the Usher protein complex are also expected to be valuable in developing therapies against this devastating hereditary human disease in the future. ■

We thank Anthony Zhang for critical editing of the manuscript.

This work in the author's laboratory was supported by grants from the Research Grants Council of Hong Kong to M. Zhang. (HKUST663808, 664009, 660709, 663610, HKUST6/CRF/10, SEG_HKUST06, and AoE/B-15/01-II). We apologize to the authors whose work cannot be cited here due to the space limitation.

No conflicts of interest, financial or otherwise, are declared by the author(s).

Author contributions: L.P. prepared figures; L.P. and M.Z. drafted the manuscript; L.P. and M.Z. edited and revised the manuscript; L.P. and M.Z. approved the final version of the manuscript.

References

1. Adato A, Michel V, Kikkawa Y, Reiners J, Alagramam KN, Weil D, Yonekawa H, Wolfrum U, El-Amraoui A, Petit C. Interactions in the network of Usher syndrome type 1 proteins. *Hum Mol Genet* 14: 347–356, 2005.
2. Ahmed ZM, Goodyear R, Riazuddin S, Lagziel A, Legan PK, Behra M, Burgess SM, Lilley KS, Wilcox ER, Griffith AJ, Frolenkov GI, Belyantseva IA, Richardson GP, Friedman TB. The tip-link antigen, a protein associated with the transduction complex of sensory hair cells, is protocadherin-15. *J Neurosci* 26: 7022–7034, 2006.
3. Ahmed ZM, Riazuddin S, Ahmad J, Bernstein SL, Guo Y, Sabar MF, Sieving P, Griffith AJ, Friedman TB, Belyantseva IA, Wilcox ER. PCDH15 is expressed in the neurosensory epithelium of the eye and ear and mutant alleles are responsible for both USH1F and DFNB23. *Hum Mol Genet* 12: 3215–3223, 2003.
4. Ahmed ZM, Riazuddin S, Bernstein SL, Ahmed Z, Khan S, Griffith AJ, Morell RJ, Friedman TB, Wilcox ER. Mutations of the protocadherin gene PCDH15 cause Usher syndrome type 1F. *Am J Hum Genet* 69: 25–34, 2001.
5. Ahmed ZM, Riazuddin S, Wilcox ER. The molecular genetics of Usher syndrome. *Clin Genet* 63: 431–444, 2003.
6. Ahmed ZM, Smith TN, Riazuddin S, Makishima T, Ghosh M, Bokhari S, Menon PS, Deshmukh D, Griffith AJ, Friedman TB, Wilcox ER. Nonsyndromic recessive deafness DFNB18 and Usher syndrome type IC are allelic mutations of USHIC. *Hum Genet* 110: 527–531, 2002.
7. Alagramam KN, Murcia CL, Kwon HY, Pawlowski KS, Wright CG, Woychik RP. The mouse Ames waltzer hearing-loss mutant is caused by mutation of Pcdh15, a novel protocadherin gene. *Nat Genet* 27: 99–102, 2001.
8. Alagramam KN, Yuan H, Kuehn MH, Murcia CL, Wayne S, Srisailpathy CR, Lowry RB, Knaus R, Van Laer L, Bernier FP, Schwartz S, Lee C, Morton CC, Mullins RF, Ramesh A, Van Camp G, Hageman GS, Woychik RP, Smith RJ. Mutations in the novel protocadherin PCDH15 cause Usher syndrome type 1F. *Hum Mol Genet* 10: 1709–1718, 2001.
9. Appler JM, Goodrich LV. Connecting the ear to the brain: molecular mechanisms of auditory circuit assembly. *Prog Neurobiol* 93: 488–508, 2011.
10. Auer M, Koster AJ, Ziese U, Bajaj C, Volkmann N, Wang da N, Hudspeth AJ. Three-dimensional architecture of hair-bundle linkages revealed by electron-microscopic tomography. *J Assoc Res Otolaryngol* 9: 215–224, 2008.

11. Bahloul A, Michel V, Hardelin JP, Nouaille S, Hoos S, Houdusse A, England P, Petit C. Cadherin-23, myosin VIIa and harmonin, encoded by Usher syndrome type I genes, form a ternary complex and interact with membrane phospholipids. *Hum Mol Genet* 19: 3557–3565, 2010.

12. Bell GI. Models for the specific adhesion of cells to cells. *Science* 200: 618–627, 1978.

13. Beurg M, Fettiplace R, Nam JH, Ricci AJ. Localization of inner hair cell mechanotransducer channels using high-speed calcium imaging. *Nat Neurosci* 12: 553–558, 2009.

14. Bitner-Glindzicz M, Lindley KJ, Rutland P, Blaydon D, Smith VV, Milla PJ, Hussain K, Furth-Lavi J, Cosgrove KE, Shepherd RM, Barnes PD, O'Brien RE, Farndon PA, Sowden J, Liu XZ, Scanlan MJ, Malcolm S, Dunne MJ, Aynsley-Green A, Glaser B. A recessive contiguous gene deletion causing infantile hyperinsulinism, enteropathy and deafness identifies the Usher type 1C gene. *Nat Genet* 26: 56–60, 2000.

15. Boeda B, El-Amraoui A, Bahloul A, Goodyear R, Daviet L, Blanchard S, Perfettini I, Fath KR, Shorte S, Reiners J, Houdusse A, Legrain P, Wolfrum U, Richardson G, Petit C. Myosin VIIa, harmonin and cadherin 23, three Usher I gene products that cooperate to shape the sensory hair cell bundle. *EMBO J* 21: 6689–6699, 2002.

16. Boggon TJ, Murray J, Chappuis-Flament S, Wong E, Gumbiner BM, Shapiro L. C-cadherin ectodomain structure and implications for cell adhesion mechanisms. *Science* 296: 1308–1313, 2002.

17. Bolz H, von Brederlow B, Ramirez A, Bryda EC, Kutsche K, Nothwang HG, Seeliger M, del CSCM, Vila MC, Molina OP, Gal A, Kubisch C. Mutation of CDH23, encoding a new member of the cadherin gene family, causes Usher syndrome type 1D. *Nat Genet* 27: 108–112, 2001.

18. Bork JM, Peters LM, Riazuddin S, Bernstein SL, Ahmed ZM, Ness SL, Polomeno R, Ramesh A, Schloss M, Srisailpathy CR, Wayne S, Bellman S, Desmukh D, Ahmed Z, Khan SN, Kaloustian VM, Li XC, Lalwani A, Bitner-Glindzicz M, Nance WE, Liu XZ, Wistow G, Smith RJ, Griffith AJ, Wilcox ER, Friedman TB, Morell RJ. Usher syndrome 1D and nonsyndromic autosomal recessive deafness DFNB12 are caused by allelic mutations of the novel cadherin-like gene CDH23. *Am J Hum Genet* 68: 26–37, 2001.

19. Boughman JA, Vernon M, Shaver KA. Usher syndrome: definition and estimate of prevalence from two high-risk populations. *J Chronic Dis* 36: 595–603, 1983.

20. Caberlotto E, Michel V, Foucher I, Bahloul A, Goodyear RJ, Pepermans E, Michalski N, Perfettini I, Alegria-Prevot O, Chardenoux S, Do Cruzeiro M, Hardelin JP, Richardson GP, Avan P, Weil D, Petit C. Usher type 1G protein sans is a critical component of the tip-link complex, a structure controlling actin polymerization in stereocilia. *Proc Natl Acad Sci USA* 108: 5825–5830, 2011.

21. Corey DP, Hudspeth AJ. Kinetics of the receptor current in bullfrog saccular hair cells. *J Neurosci* 3: 962–976, 1983.

22. Craven SE, Bredt DS. PDZ proteins organize synaptic signaling pathways. *Cell* 93: 495–498, 1998.

23. Di Palma F, Holme RH, Bryda EC, Belyantseva IA, Pellegrino R, Kachar B, Steel KP, Noben-Trauth K. Mutations in Cdh23, encoding a new type of cadherin, cause stereocilia disorganization in waltzer, the mouse model for Usher syndrome type 1D. *Nat Genet* 27: 103–107, 2001.

24. El-Amraoui A, Petit C. Usher I syndrome: unravelling the mechanisms that underlie the cohesion of the growing hair bundle in inner ear sensory cells. *J Cell Sci* 118: 4593–4603, 2005.

25. Elledge HM, Kazmierczak P, Clark P, Joseph JS, Kolatkar A, Kuhn P, Muller U. Structure of the N terminus of cadherin 23 reveals a new adhesion mechanism for a subset of cadherin superfamily members. *Proc Natl Acad Sci USA* 107: 10708–10712, 2010.

26. Etournay R, El-Amraoui A, Bahloul A, Blanchard S, Roux I, Pezeron G, Michalski N, Daviet L, Hardelin JP, Legrain P, Petit C. PHR1, an integral membrane protein of the inner ear sensory cells, directly interacts with myosin 1c and myosin VIIa. *J Cell Sci* 118: 2891–2899, 2005.

27. Etournay R, Zwaenepoel I, Perfettini I, Legrain P, Petit C, El-Amraoui A. Shroom2, a myosin-VIIa- and actin-binding protein, directly interacts with ZO-1 at tight junctions. *J Cell Sci* 120: 2838–2850, 2007.

28. Eudy JD, Weston MD, Yao S, Hoover DM, Rehm HL, Ma-Edmonds M, Yan D, Ahmad I, Cheng JJ, Ayuso C, Cremers C, Davenport S, Moller C, Talmadge CB, Beisel KW, Tamayo M, Morton CC, Swaroop A, Kimberling WJ, Sumegi J. Mutation of a gene encoding a protein with extracellular matrix motifs in Usher syndrome type IIa. *Science* 280: 1753–1757, 1998.

29. Feng W, Zhang M. Organization and dynamics of PDZ-domain-related supramodules in the postsynaptic density. *Nat Rev Neurosci* 10: 87–99, 2009.

30. Fettiplace R, Hackney CM. The sensory and motor roles of auditory hair cells. *Nat Rev Neurosci* 7: 19–29, 2006.

31. Friedman TB, Griffith AJ. Human nonsyndromic sensorineural deafness. *Annu Rev Genomics Hum Genet* 4: 341–402, 2003.

32. Friedman TB, Schultz JM, Ahmed ZM, Tsilou ET, Brewer CC. Usher syndrome: hearing loss with vision loss. *Adv Otorhinolaryngol* 70: 56–65, 2011.

33. Fritzsch B, Beisel KW, Pauley S, Soukup G. Molecular evolution of the vertebrate mechanosensory cell and ear. *Int J Dev Biol* 51: 663–678, 2007.

34. Frolenkov GI, Belyantseva IA, Friedman TB, Griffith AJ. Genetic insights into the morphogenesis of inner ear hair cells. *Nat Rev Genet* 5: 489–498, 2004.

35. Furness DN, Hackney CM. Cross-links between stereocilia in the guinea pig cochlea. *Hear Res* 18: 177–188, 1985.

36. Furness DN, Mahendrasingam S, Ohashi M, Fettiplace R, Hackney CM. The dimensions and composition of stereociliary rootlets in mammalian cochlear hair cells: comparison between high- and low-frequency cells and evidence for a connection to the lateral membrane. *J Neurosci* 28: 6342–6353, 2008.

37. Geleoc GS, Holt JR. Developmental acquisition of sensory transduction in hair cells of the mouse inner ear. *Nat Neurosci* 6: 1019–1020, 2003.

38. Gillespie PG, Muller U. Mechanotransduction by hair cells: models, molecules, and mechanisms. *Cell* 139: 33–44, 2009.

39. Gillespie PG, Walker RG. Molecular basis of mechanosensory transduction. *Nature* 413: 194–202, 2001.

40. Goodyear RJ, Forge A, Legan PK, Richardson GP. Asymmetric distribution of cadherin 23 and protocadherin 15 in the kinocilial links of avian sensory hair cells. *J Comp Neurol* 518: 4288–4297, 2010.

41. Goodyear RJ, Marcotti W, Kros CJ, Richardson GP. Development and properties of stereociliary link types in hair cells of the mouse cochlea. *J Comp Neurol* 485: 75–85, 2005.

42. Grati M, Kachar B. Myosin VIIa and sans localization at stereocilia upper tip-link density implicates these Usher syndrome proteins in mechanotransduction. *Proc Natl Acad Sci USA* 108: 11476–11481, 2011.

43. Gregory FD, Bryan KE, Pangrsic T, Calin-Jageman IE, Moser T, Lee A. Harmonin inhibits presynaptic $Ca_v1.3$ Ca^{2+} channels in mouse inner hair cells. *Nat Neurosci* 14: 1109–1111, 2011.

44. Grillet N, Xiong W, Reynolds A, Kazmierczak P, Sato T, Lillo C, Dumont RA, Hintermann E, Sczaniecka A, Schwander M, Williams D, Kachar B, Gillespie PG, Muller U. Harmonin mutations cause mechanotransduction defects in cochlear hair cells. *Neuron* 62: 375–387, 2009.

45. Haithcock J, Billington N, Choi K, Fordham J, Sellers JR, Stafford WF, White H, Forgacs E. The kinetic mechanism of mouse myosin VIIA. *J Biol Chem* 286: 8819–8828, 2011.

46. Hampton LL, Wright CG, Alagramam KN, Battey JF, Noben-Trauth K. A new spontaneous mutation in the mouse Ames waltzer gene, *Pcdh15*. *Hear Res* 180: 67–75, 2003.

47. Hasson T, Gillespie PG, Garcia JA, MacDonald RB, Zhao Y, Yee AG, Mooseker MS, Corey DP. Unconventional myosins in inner-ear sensory epithelia. *J Cell Biol* 137: 1287–1307, 1997.

48. Hasson T, Heintzelman MB, Santos-Sacchi J, Corey DP, Mooseker MS. Expression in cochlea and retina of myosin VIIa, the gene product defective in Usher syndrome type 1B. *Proc Natl Acad Sci USA* 92: 9815–9819, 1995.

49. Hilgert N, Smith RJ, Van Camp G. Function and expression pattern of nonsyndromic deafness genes. *Curr Mol Med* 9: 546–564, 2009.

50. Hirano Y, Hatano T, Takahashi A, Toriyama M, Inagaki N, Hakoshima T. Structural basis of cargo recognition by the myosin-X MyTH4-FERM domain. *EMBO J* 30: 2734–2747, 2011.

51. Howard J, Hudspeth AJ. Compliance of the hair bundle associated with gating of mechanoelectrical transduction channels in the bullfrog's saccular hair cell. *Neuron* 1: 189–199, 1988.

52. Hudspeth AJ. How the ear's works work. *Nature* 341: 397–404, 1989.

53. Hudspeth AJ. Making an effort to listen: mechanical amplification in the ear. *Neuron* 59: 530–545, 2008.

54. Inoue A, Ikebe M. Characterization of the motor activity of mammalian myosin VIIA. *J Biol Chem* 278: 5478–5487, 2003.

55. Joensuu T, Hamalainen R, Yuan B, Johnson C, Tegelberg S, Gasparini P, Zelante L, Pirvola U, Pakarinen L, Lehesjoki AE, de la Chapelle A, Sankila EM. Mutations in a novel gene with transmembrane domains underlie Usher syndrome type 3. *Am J Hum Genet* 69: 673–684, 2001.

56. Johnson KR, Gagnon LH, Webb LS, Peters LL, Hawes NL, Chang B, Zheng QY. Mouse models of USH1C and DFNB18: phenotypic and molecular analyses of two new spontaneous mutations of the Ush1c gene. *Hum Mol Genet* 12: 3075–3086, 2003.

57. Kazmierczak P, Sakaguchi H, Tokita J, Wilson-Kubalek EM, Milligan RA, Muller U, Kachar B. Cadherin 23 and protocadherin 15 interact to form tip-link filaments in sensory hair cells. *Nature* 449: 87–91, 2007.

58. Kelly M, Chen P. Shaping the mammalian auditory sensory organ by the planar cell polarity pathway. *Int J Dev Biol* 51: 535–547, 2007.

59. Kikkawa Y, Shitara H, Wakana S, Kohara Y, Takada T, Okamoto M, Taya C, Kamiya K, Yoshikawa Y, Tokano H, Kitamura K, Shimizu K, Wakabayashi Y, Shiroishi T, Kominami R, Yonekawa H. Mutations in a new scaffold protein Sans cause deafness in Jackson shaker mice. *Hum Mol Genet* 12: 453–461, 2003.

60. Kitajiri S, Sakamoto T, Belyantseva IA, Goodyear RJ, Stepanyan R, Fujiwara I, Bird JE, Riazuddin S, Ahmed ZM, Hinshaw JE, Sellers J, Bartles JR, Hammer JA, 3rd Richardson GP, Griffith AJ, Frolenkov GI, Friedman TB. Actin-bundling protein TRIOBP forms resilient rootlets of hair cell stereocilia essential for hearing. *Cell* 141: 786–798, 2010.

61. Knight PJ, Thirumurugan K, Xu Y, Wang F, Kalverda AP, Stafford WF, 3rd Sellers JR, Peckham M. The predicted coiled-coil domain of myosin 10 forms a novel elongated domain that lengthens the head. *J Biol Chem* 280: 34702–34708, 2005.

62. Kozlov AS, Baumgart J, Risler T, Versteegh CP, Hudspeth AJ. Forces between clustered stereocilia minimize friction in the ear on a subnanometre scale. *Nature* 474: 376–379, 2011.

63. Kozlov AS, Risler T, Hudspeth AJ. Coherent motion of stereocilia assures the concerted gating of hair-cell transduction channels. *Nat Neurosci* 10: 87–92, 2007.

64. Kremer H, van Wijk E, Marker T, Wolfrum U, Roepman R. Usher syndrome: molecular links of pathogenesis, proteins and pathways. *Hum Mol Genet* 15, *Spec No* 2: R262–R270, 2006.

65. Kros CJ, Marcotti W, van Netten SM, Self TJ, Libby RT, Brown SD, Richardson GP, Steel KP. Reduced climbing and increased slipping adaptation in cochlear hair cells of mice with Myo7a mutations. *Nat Neurosci* 5: 41–47, 2002.

66. Kuroda TS, Fukuda M. Functional analysis of Slac2-c/MyRIP as a linker protein between melanosomes and myosin VIIa. *J Biol Chem* 280: 28015–28022, 2005.

67. Lagziel A, Ahmed ZM, Schultz JM, Morell RJ, Belyantseva IA, Friedman TB. Spatiotemporal pattern and isoforms of cadherin 23 in wild type and waltzer mice during inner ear hair cell development. *Dev Biol* 280: 295–306, 2005.

68. Lefevre G, Michel V, Weil D, Lepelletier L, Bizard E, Wolfrum U, Hardelin JP, Petit C. A core cochlear phenotype in USH1 mouse mutants implicates fibrous links of the hair bundle in its cohesion, orientation and differential growth. *Development* 135: 1427–1437, 2008.

69. Li J, Mahajan A, Tsai MD. Ankyrin repeat: a unique motif mediating protein-protein interactions. *Biochemistry* 45: 15168–15178, 2006.

70. Liu XZ, Walsh J, Mburu P, Kendrick-Jones J, Cope MJ, Steel KP, Brown SD. Mutations in the myosin VIIA gene cause non-syndromic recessive deafness. *Nat Genet* 16: 188–190, 1997.

71. Maniak M. Cell adhesion: ushering in a new understanding of myosin VII. *Curr Biol* 11: R315–R317, 2001.

72. Mburu P, Mustapha M, Varela A, Weil D, El-Amraoui A, Holme RH, Rump A, Hardisty RE, Blanchard S, Coimbra RS, Perfettini I, Parkinson N, Mallon AM, Glenister P, Rogers MJ, Paige AJ, Moir L, Clay J, Rosenthal A, Liu XZ, Blanco G, Steel KP, Petit C, Brown SD. Defects in whirlin, a PDZ domain molecule involved in stereocilia elongation, cause deafness in the whirler mouse and families with DFNB31. *Nat Genet* 34: 421–428, 2003.

73. Michel V, Goodyear RJ, Weil D, Marcotti W, Perfettini I, Wolfrum U, Kros CJ, Richardson GP, Petit C. Cadherin 23 is a component of the transient lateral links in the developing hair bundles of cochlear sensory cells. *Dev Biol* 280: 281–294, 2005.

74. Millan JM, Aller E, Jaijo T, Blanco-Kelly F, Gimenez-Pardo A, Ayuso C. An update on the genetics of usher syndrome. *J Ophthalmol* 2011: 417217, 2011.

75. Moen RJ, Johnsrud DO, Thomas DD, Titus MA. Characterization of a myosin VII MyTH/FERM domain. *J Mol Biol* 413: 17–23, 2011.

76. Muller U. Cadherins and mechanotransduction by hair cells. *Curr Opin Cell Biol* 20: 557–566, 2008.

77. Nayak GD, Ratnayaka HS, Goodyear RJ, Richardson GP. Development of the hair bundle and mechanotransduction. *Int J Dev Biol* 51: 597–608, 2007.

78. Ouyang XM, Xia XJ, Verpy E, Du LL, Pandya A, Petit C, Balkany T, Nance WE, Liu XZ. Mutations in the alternatively spliced exons of USH1C cause non-syndromic recessive deafness. *Hum Genet* 111: 26–30, 2002.

79. Pan L, Yan J, Wu L, Zhang M. Assembling stable hair cell tip link complex via multidentate interactions between harmonin and cadherin 23. *Proc Natl Acad Sci USA* 106: 5575–5580, 2009.

80. Patel SD, Ciatto C, Chen CP, Bahna F, Rajebhosale M, Arkus N, Schieren I, Jessell TM, Honig B, Price SR, Shapiro L. Type II cadherin ectodomain structures: implications for classical cadherin specificity. *Cell* 124: 1255–1268, 2006.

81. Pennings RJ, Kremer H, Deutman AF, Kimberling WJ, Cremers CW. [From gene to disease; genetic causes of hearing loss and visual impairment sometimes accompanied by vestibular problems (Usher syndrome)]. *Ned Tijdschr Geneeskd* 146: 2354–2358, 2002.

82. Petit C. Usher syndrome: from genetics to pathogenesis. *Annu Rev Genomics Hum Genet* 2: 271–297, 2001.

83. Petit C, Richardson GP. Linking genes underlying deafness to hair-bundle development and function. *Nat Neurosci* 12: 703–710, 2009.

84. Pickles JO, Comis SD, Osborne MP. Cross-links between stereocilia in the guinea pig organ of Corti, and their possible relation to sensory transduction. *Hear Res* 15: 103–112, 1984.

85. Pokutta S, Weis WI. Structure and mechanism of cadherins and catenins in cell-cell contacts. *Annu Rev Cell Dev Biol* 23: 237–261, 2007.

86. Qiao F, Bowie JU. The many faces of SAM. *Sci STKE* 2005: re7, 2005.

87. Reiners J, Marker T, Jurgens K, Reidel B, Wolfrum U. Photoreceptor expression of the Usher syndrome type 1 protein protocadherin 15 (USH1F) and its interaction with the scaffold protein harmonin (USH1C). *Mol Vis* 11: 347–355, 2005.

88. Reiners J, Nagel-Wolfrum K, Jurgens K, Marker T, Wolfrum U. Molecular basis of human Usher syndrome: deciphering the meshes of the Usher protein network provides insights into the pathomechanisms of the Usher disease. *Exp Eye Res* 83: 97–119, 2006.

89. Reiners J, Reidel B, El-Amraoui A, Boeda B, Huber I, Petit C, Wolfrum U. Differential distribution of harmonin isoforms and their possible role in Usher-1 protein complexes in mammalian photoreceptor cells. *Invest Ophthalmol Vis Sci* 44: 5006–5015, 2003.

90. Reiners J, van Wijk E, Marker T, Zimmermann U, Jurgens K, te Brinke H, Overlack N, Roepman R, Knipper M, Kremer H, Wolfrum U. Scaffold protein harmonin (USH1C) provides molecular links between Usher syndrome type 1 and type 2. *Hum Mol Genet* 14: 3933–3943, 2005.

91. Reiners J, Wolfrum U. Molecular analysis of the supramolecular usher protein complex in the retina. Harmonin as the key protein of the Usher syndrome. *Adv Exp Med Biol* 572: 349–353, 2006.

92. Richardson GP, de Monvel JB, Petit C. How the genetics of deafness illuminates auditory physiology. *Annu Rev Physiol* 73: 311–334, 2011.

93. Roepman R, Wolfrum U. Protein networks and complexes in photoreceptor cilia. *Subcell Biochem* 43: 209–235, 2007.

94. Rosenberg T, Haim M, Hauch AM, Parving A. The prevalence of Usher syndrome and other retinal dystrophy-hearing impairment associations. *Clin Genet* 51: 314–321, 1997.

95. Sakai T, Umeki N, Ikebe R, Ikebe M. Cargo binding activates myosin VIIA motor function in cells. *Proc Natl Acad Sci USA* 108: 7028–7033, 2011.

96. Self T, Mahony M, Fleming J, Walsh J, Brown SD, Steel KP. Shaker-1 mutations reveal roles for myosin VIIA in both development and function of cochlear hair cells. *Development* 125: 557–566, 1998.

97. Senften M, Schwander M, Kazmierczak P, Lillo C, Shin JB, Hasson T, Geleoc GS, Gillespie PG, Williams D, Holt JR, Muller U. Physical and functional interaction between protocadherin 15 and myosin VIIa in mechanosensory hair cells. *J Neurosci* 26: 2060–2071, 2006.

98. Shapiro L, Weis WI. Structure and biochemistry of cadherins and catenins. *Cold Spring Harb Perspect Biol* 1: a003053, 2009.

99. Siemens J, Kazmierczak P, Reynolds A, Sticker M, Littlewood-Evans A, Muller U. The Usher syndrome proteins cadherin 23 and harmonin form a complex by means of PDZ-domain interactions. *Proc Natl Acad Sci USA* 99: 14946–14951, 2002.

100. Siemens J, Lillo C, Dumont RA, Reynolds A, Williams DS, Gillespie PG, Muller U. Cadherin 23 is a component of the tip link in hair-cell stereocilia. *Nature* 428: 950–955, 2004.

101. Sotomayor M, Weihofen WA, Gaudet R, Corey DP. Structural determinants of cadherin-23 function in hearing and deafness. *Neuron* 66: 85–100, 2010.

102. Sousa S, Cabanes D, El-Amraoui A, Petit C, Lecuit M, Cossart P. Unconventional myosin VIIa and vezatin, two proteins crucial for Listeria entry into epithelial cells. *J Cell Sci* 117: 2121–2130, 2004.

103. Steinberg MS, McNutt PM. Cadherins and their connections: adhesion junctions have broader functions. *Curr Opin Cell Biol* 11: 554–560, 1999.

104. Tlili A, Charfedine I, Lahmar I, Benzina Z, Mohamed BA, Weil D, Idriss N, Drira M, Masmoudi S, Ayadi H. Identification of a novel frameshift mutation in the DFNB31/WHRN gene in a Tunisian consanguineous family with hereditary nonsyndromic recessive hearing loss. *Hum Mutat* 25: 503, 2005.

105. Umeki N, Jung HS, Watanabe S, Sakai T, Li XD, Ikebe R, Craig R, Ikebe M. The tail binds to the head-neck domain, inhibiting ATPase activity of myosin VIIA. *Proc Natl Acad Sci USA* 106: 8483–8488, 2009.

106. van Wijk E, Pennings RJ, te Brinke H, Claassen A, Yntema HG, Hoefsloot LH, Cremers FP, Cremers CW, Kremer H. Identification of 51 novel exons of the Usher syndrome type 2A (*USH2A*) gene that encode multiple conserved functional domains and that are mutated in patients with Usher syndrome type II. *Am J Hum Genet* 74: 738–744, 2004.

107. Verpy E, Leibovici M, Zwaenepoel I, Liu XZ, Gal A, Salem N, Mansour A, Blanchard S, Kobayashi I, Keats BJ, Slim R, Petit C. A defect in harmonin, a PDZ domain-containing protein expressed in the inner ear sensory hair cells, underlies Usher syndrome type 1C. *Nat Genet* 26: 51–55, 2000.

108. Verpy E, Weil D, Leibovici M, Goodyear RJ, Hamard G, Houdon C, Lefevre GM, Hardelin JP, Richardson GP, Avan P, Petit C. Stereocilin-deficient mice reveal the origin of cochlear waveform distortions. *Nature* 456: 255–258, 2008.

109. Vollrath MA, Kwan KY, Corey DP. The micromachinery of mechanotransduction in hair cells. *Annu Rev Neurosci* 30: 339–365, 2007.

110. Vrijens K, Van Laer L, Van Camp G. Human hereditary hearing impairment: mouse models can help to solve the puzzle. *Hum Genet* 124: 325–348, 2008.

111. Webb SW, Grillet N, Andrade LR, Xiong W, Swarthout L, Della Santina CC, Kachar B, Muller U. Regulation of PCDH15 function in mechanosensory hair cells by alternative splicing of the cytoplasmic domain. *Development* 138: 1607–1617, 2011.

112. Wei Z, Yan J, Lu Q, Pan L, Zhang M. Cargo recognition mechanism of myosin X revealed by the structure of its tail MyTH4-FERM tandem in complex with the DCC P3 domain. *Proc Natl Acad Sci USA* 108: 3572–3577, 2011.

113. Weil D, Blanchard S, Kaplan J, Guilford P, Gibson F, Walsh J, Mburu P, Varela A, Levilliers J, Weston MD, et al. Defective myosin VIIA gene responsible for Usher syndrome type 1B. *Nature* 374: 60–61, 1995.

114. Weil D, El-Amraoui A, Masmoudi S, Mustapha M, Kikkawa Y, Laine S, Delmaghani S, Adato A, Nadifi S, Zina ZB, Hamel C, Gal A, Ayadi H, Yonekawa H, Petit C. Usher syndrome type I G (USH1G) is caused by mutations in the gene encoding SANS, a protein that associates with the USH1C protein, harmonin. *Hum Mol Genet* 12: 463–471, 2003.

115. Weil D, Levy G, Sahly I, Levi-Acobas F, Blanchard S, El-Amraoui A, Crozet F, Philippe H, Abitbol M, Petit C. Human myosin VIIA responsible for the Usher 1B syndrome: a predicted membrane-associated motor protein expressed in developing sensory epithelia. *Proc Natl Acad Sci USA* 93: 3232–3237, 1996.

116. Weston MD, Eudy JD, Fujita S, Yao S, Usami S, Cremers C, Greenberg J, Ramesar R, Martini A, Moller C, Smith RJ, Sumegi J, Kimberling WJ. Genomic structure and identification of novel mutations in usherin, the gene responsible for Usher syndrome type IIa. *Am J Hum Genet* 66: 1199–1210, 2000.

117. Weston MD, Luijendijk MW, Humphrey KD, Moller C, Kimberling WJ. Mutations in the VLGR1 gene implicate G-protein signaling in the pathogenesis of Usher syndrome type II. *Am J Hum Genet* 74: 357–366, 2004.

118. Wheelock MJ, Johnson KR. Cadherins as modulators of cellular phenotype. *Annu Rev Cell Dev Biol* 19: 207–235, 2003.

119. Williams DS. Usher syndrome: animal models, retinal function of Usher proteins, and prospects for gene therapy. *Vision Res* 48: 433–441, 2008.

120. Wilson SM, Householder DB, Coppola V, Tessarollo L, Fritzsch B, Lee EC, Goss D, Carlson GA, Copeland NG, Jenkins NA. Mutations in Cdh23 cause nonsyndromic hearing loss in waltzer mice. *Genomics* 74: 228–233, 2001.

121. Wolfrum U. The cellular function of the usher gene product myosin VIIa is specified by its ligands. *Adv Exp Med Biol* 533: 133–142, 2003.

122. Wu L, Pan L, Wei Z, Zhang M. Structure of MyTH4-FERM domains in myosin VIIa tail bound to cargo. *Science* 331: 757–760, 2011.

123. Xu Z, Peng AW, Oshima K, Heller S. MAGI-1, a candidate stereociliary scaffolding protein, associates with the tip-link component cadherin 23. *J Neurosci* 28: 11269–11276, 2008.

124. Yan D, Kamiya K, Ouyang XM, Liu XZ. Analysis of subcellular localization of Myo7a, Pcdh15 and Sans in Ush1c knockout mice. *Int J Exp Pathol* 92: 66–71, 2011.

125. Yan D, Liu XZ. Genetics and pathological mechanisms of Usher syndrome. *J Hum Genet* 55: 327–335, 2010.

126. Yan J, Pan L, Chen X, Wu L, Zhang M. The structure of the harmonin/sans complex reveals an unexpected interaction mode of the two Usher syndrome proteins. *Proc Natl Acad Sci USA* 107: 4040–4045, 2010.

127. Yang Y, Baboolal TG, Siththanandan V, Chen M, Walker ML, Knight PJ, Peckham M, Sellers JR. A FERM domain autoregulates *Drosophila* myosin 7a activity. *Proc Natl Acad Sci USA* 106: 4189–4194, 2009.

128. Yang Y, Kovacs M, Sakamoto T, Zhang F, Kiehart DP, Sellers JR. Dimerized Drosophila myosin VIIa: a processive motor. *Proc Natl Acad Sci USA* 103: 5746–5751, 2006.

129. Yu C, Feng W, Wei Z, Miyanoiri Y, Wen W, Zhao Y, Zhang M. Myosin VI undergoes cargo-mediated dimerization. *Cell* 138: 537–548, 2009.

130. Zhang M, Wang W. Organization of signaling complexes by PDZ-domain scaffold proteins. *Acc Chem Res* 36: 530–538, 2003.

131. Zheng L, Zheng J, Whitlon DS, Garcia-Anoveros J, Bartles JR. Targeting of the hair cell proteins cadherin 23, harmonin, myosin XVa, espin, and prestin in an epithelial cell model. *J Neurosci* 30: 7187–7201, 2010.